Res. Rep. Fac. Eng. Mie Univ., Vol. 28, pp. 25−60 (2003)

Original Paper

Research and Construction of the Concrete-Filled Steel Tube Column System in Japan

Shosuke Morino and Jun Kawaguchi
Department of Architecture

(Received September 16, 2003)

ABSTRACT

The concrete-filled steel tube (CFT) column system has many advantages compared with the ordinary steel or the reinforced concrete system. One of the main advantages is the interaction between steel tube and concrete: local buckling of steel tube is delayed by the restraint of concrete, the strength of concrete is increased by the confining effect of the steel tube. Extensive research works have been done in Japan last 15 years, including the "New Urban Housing Project"and the "US-Japan Cooperative Earthquake Research Program", in addition to the works done by individual universities and industries that have been presented at the annual meetings of Architectural Institute of Japan (AIJ). Mie University has also been contributing to the development of the CFT column system in a great extent. This paper introduces the structural system and discusses advantages, research findings, trial designs, and recent construction trends of CFT column system in Japan. The paper also describes the design recommendations for the design of compression members, beam-columns, and beam-to-column connections in the CFT column system.

Keywords: CFT column system, Overview, Research, Construction, Design provisions

1. INTRODUCTION

Since 1970, extensive investigations have verified that framing systems consisting of concrete-filled steel tube (CFT) columns and H-shaped beams have more benefit than ordinary reinforced concrete and steel systems, and as a result, this system has very frequently been utilized in the construction of middle- and high-rise buildings in Japan. Typical connections between a CFT column and H-shaped beams often used in Japan are shown in Fig. 1. The connection is fabricated by shop welding, and the beams are bolted to the brackets onsite. In the case of connections using inner and through-type diaphragms, the diaphragm plates are located inside the tube, and a hole is opened for concrete casting. A cast steel ring stiffener is used for a circular CFT column. In the case of a ring stiffener and an outer diaphragm, there is no object inside the tube to interfere with the smooth casting of the concrete. Bare and embedded type column bases shown in Fig. 2 are usually used in the CFT column system, and the structural reliability of the latter is much higher than that of the former. When the building has the basement stories, the CFT column section is converted to the concrete encased cross-H section at the first story of the basement as shown in Fig. 2 in some cases.

Concrete casting is usually done by Tremie tube or the pump-up method. High strength and ductility can be obtained in the CFT column system because of the advantages mentioned below. However, difficulty in properly compacting the concrete may create a weak point in the system, especially in the case of inner and through-type diaphragms where bleeding of the concrete beneath the diaphragm may produce a gap between the concrete and steel. There is currently no way to ensure compactness or to repair this deficiency. To compensate, high-quality concrete with a low water content and a superplasticizer for enhanced workability are used in construction.

This paper first describes the advantages of the CFT column system in view of structural performance and constructional efficiency, introduces the summary of research and design provisions, discusses the cost merits of the CFT column system investigated by the trial designs of the theme structures, and finally the recent trends of the construction of CFT column system in Japan.

2. ADVANTAGES OF CFT COLUMN SYSTEM

CFT column system has many advantages compared with ordinary steel or reinforced concrete systems. Main advantages are listed below:

Interaction between steel tube and concrete

1) Local buckling of the steel tube is delayed, and the strength deterioration after the local buckling is moderated, both

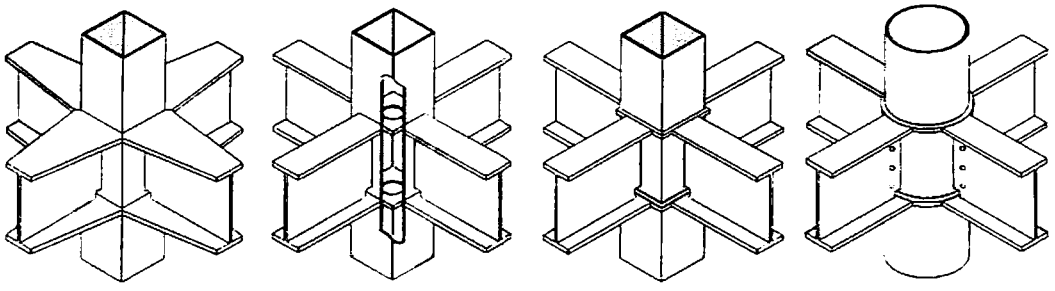

Fig. 1 Beam-to-Column Connections

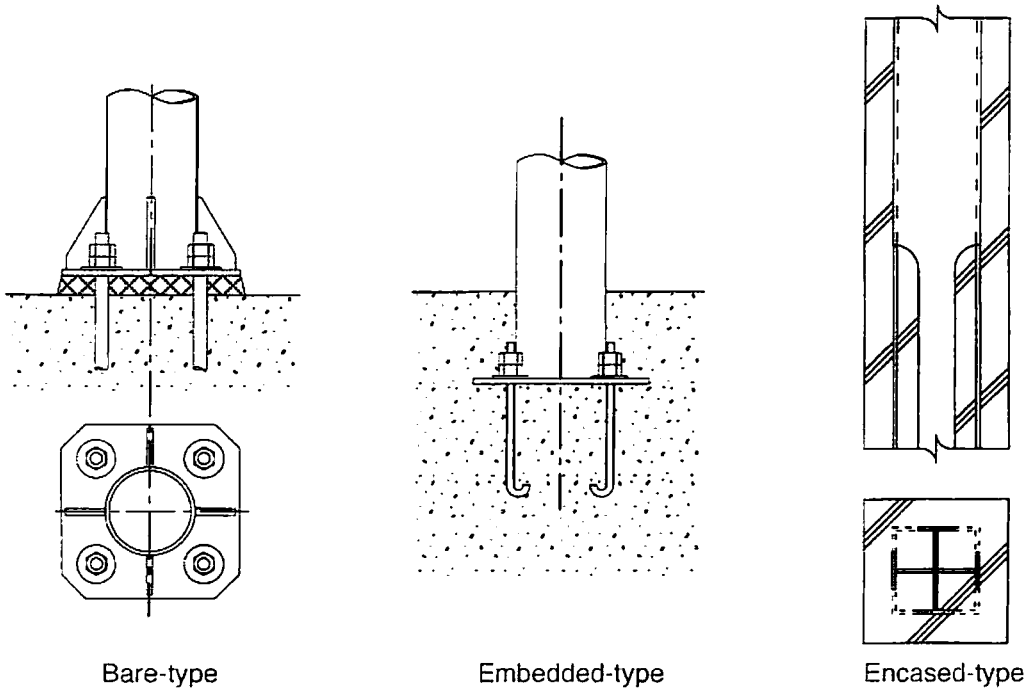

Fig. 2 Column Bases

due to the restraining effect of concrete.
2) The strength of concrete is increased due to the confining effect provided by the steel tube, and the strength deterioration is not very severe, because concrete spalling is prevented by the tube.
3) Drying shrinkage and creep of the concrete are much smaller than in ordinary reinforced concrete.

Cross-sectional properties
4) The steel ratio in the CFT cross section is much larger than in the reinforced concrete and concrete-encased steel cross sections.
5) The steel of the CFT section is well plastified under bending because it is located most outside the section.

Construction efficiency
6) Labor for forms and reinforcing bars is omitted, and concrete casting is done by Tremie tube or the pump-up method. This efficiency leads to a reduction in manpower, constructional cost, and project length.
7) Construction site becomes clean.

Fire resistance
8) Concrete improves fire resistance so that fireproof material can be reduced or omitted.

Cost performance
9) Because of the merits listed above, better cost performance is obtained by replacing a steel structure with a CFT structure.

Ecology
10) The environmental burden can be reduced by omitting the formwork and by reusing steel tubes and using high-quality concrete as recycled aggregates.

The cost advantage of the CFT column system against the steel system will be discussed later in more details.

3. RESEARCH ON CFT COLUMN SYSTEM

3.1 Research Activities

3.1.1 Architectural Institute of Japan

Figure 3 shows the number of abstracts of technical papers on composite concrete and steel structures and on the CFT column system, which have been presented at the annual meetings of Architectural Institute of Japan (AIJ). In 1961, Naka, Kato, *et al.*, wrote the first technical paper on CFT in Japan. It discussed a circular CFT compression member used in a power transmission tower. The number of abstracts presented at AIJ's annual meetings was about 10 or less every year until 1986.

The research topics treated in the papers presented at the annual meetings of AIJ are tabulated in Table 1, and summarized as follows: i) structural mechanics (stiffness, strength, post-local buckling behavior, confining effect, stress transfer mechanisms, and ductility of columns, beam-columns and beam-to-column connections); ii) construction efficiency (concrete compaction, concrete mixture, concrete casting method and construction time); iii) fire resistance (strength under fire and amount of fireproof material); and iv) structural planning (application to high-rise and long-span buildings, and cost performance).

The first edition of the AIJ standard for composite concrete and circular steel tube structures was published in 1967, based on the research carried out in the early 1960's. This edition was written for three types of circular composite sections: the so-called concrete-encased tube, the CFT and the concrete-encased and filled tube sections. The standard was revised in 1980 to include sections using square tubes. This standard was absorbed into the AIJ standard for composite concrete and steel (SRC) structures in 1987, which included the formulas to evaluate the ultimate strength of circular and square CFT columns, beam-columns and beam-to-column connections. The English version of this

standard is available at AIJ[1]. The newest edition of the SRC Standard of AIJ[2] was published in 2001. This edition increased the upper limit of the design standard strength of normal concrete to 60 MPa, and revised several parts of design provisions for the CFT column system, in accordance with the contents of the CFT Recommendations[3] explained below.

CFT Recommendations[3] were published by AIJ in 1997, based on recent research developments on the following topics. i) special types of CFT members such as braces and truss members, in addition to compression members, beam-columns and connections; ii) formulas to evaluate deformation capacity of CFT columns and frames; iii) structural characteristics under fire; iv) manufacturing of steel tube and mixture of concrete; v) analysis of the behavior of CFT columns and frames; and vi) strength formulas used in the world. Provisions for the design of CFT columns shown in the 2001 edition of the SRC Standard of AIJ[2] will be introduced in this paper later.

3.1.2 New Urban Housing Project

In 1985, five general contractors and a steel manufacturer won the Japan's Ministry of Construction proposal competition for the construction of urban apartment houses in the 21st century. Since then, these industries and the Building Research Institute (BRI) of the Ministry of Construction started a five-year experimental research project called New Urban Housing Project (NUHP), which accelerated the investigation of this system. In this project, a total of 86 specimens of centrally-loaded stub columns and beam-columns were tested under combined compression, bending and shear. Table 2 shows the number of specimens and test parameters. A sharp increase in the number of abstracts on the CFT system observed at 1987 in Fig. 3 is due to the research related to NUHP.

The results of investigation carried out under NUHP were published in CFT Reports[4], and have been used for the design of the CFT system. This report is the first document in Japan that measured the strength increase of the

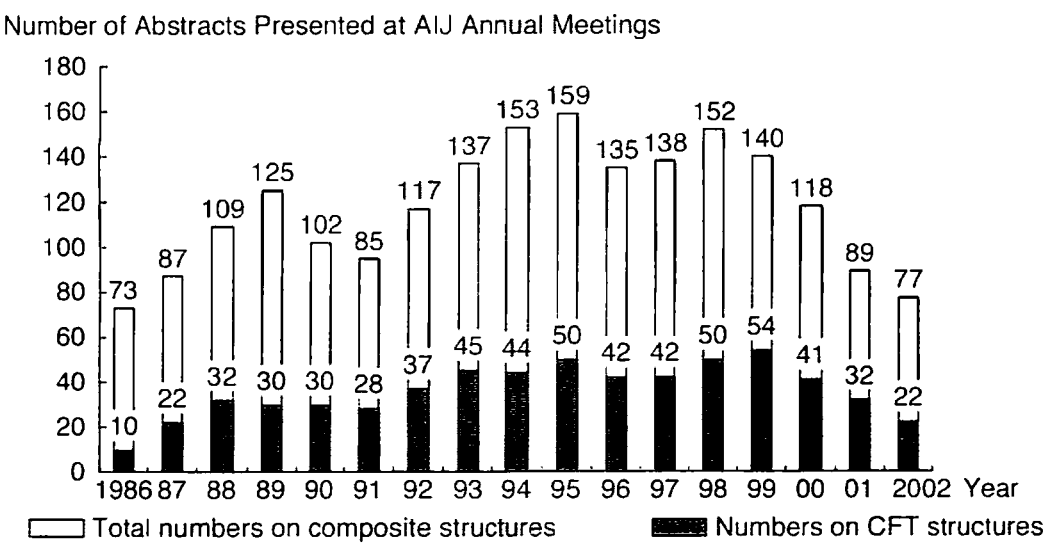

Fig. 3 Number of Abstracts Presented at AIJ Annual Meetings

Table 1 Research Items in Abstracts at AIJ Annual Meetings

Structural Mechanics	Constructional Efficiency	Fire Resistance	Structural Planning
Axial load carrying capacity	Compactness of concrete	Strength under fire	Application to high-rize building
Flexural strength	Concrete mixture	Amount of fire-proof material	Application to long-span building
Buckling strength	Concrete casting method		
Deformation capacity	Reduction of construction time		
Stiffness			
Post-local buckling behavior			
Confining effect			
Stress transfer mechanism at beam-to-column connection			

confined concrete of circular CFT members, and showed formulas to evaluate the deformation capacity. Evaluation of the deformation capacity of CFT beam-columns is needed to calculate the structural characteristic factor D_s used in seismic design. In 1996, those industries that originally joined NUHP established the Association of New Urban Housing Technology (ANUHT). The ANUHT consists of more than 100 member companies involved in CFT building construction and authorizes the structural design of newly planned CFT buildings in accordance with the ANUHT's CFT Recommendations[5]. Based on ANUHT's CFT Recommendations[5], CFT construction technology was initiated in 2002 by the publication of Notification No. 464 by the Ministry of Land, Infrastructure and Transport, Japan, and ANUHT's CFT Recommendations[5] that were closely used by the member companies was generally opened for the public use.

3.1.3 U.S.-Japan Cooperative Earthquake Research Program

A five-year research project on composite and hybrid structures started in 1993 as the fifth phase of the U.S.-Japan Cooperative Earthquake Research Program, and the program was organized into the following four groups: CFT column system; reinforced concrete column + steel beam system; hybrid wall system; and new materials, elements and systems. The program of the Japanese side for the CFT system consists of the following topics: i) experimental study; ii) database; and iii) trial design. Centrally-loaded stub columns, eccentrically loaded stub columns, beam-columns, and beam-to-column connections were tested to clarify the synergistic interaction between steel tube and concrete and stress transfer mechanism, and to derive methods to evaluate stiffness, strength and ductility of CFT elements and systems. The number of specimens and test parameters are shown in Fig. 4 and Table 2. The unique feature of this test program was that it covered the high-strength materials, such as 800 MPa steel and 90 MPa concrete, it covered large width-thickness ratio, and some of the beam-column specimens were tested under the variable axial load. Test data

Table 2 Scope of Research Projects on CFT Column System

Project	New Urban Housing Project	U.S.-Japan Cooperative Project
Shape of tube	□ ○	□ ○
Number of specimens	Centrally-loaded stub columns □: 24 ○: 24 Beam-columns under combined load □: 19 ○: 19	Centrally-loaded stub columns □: 45 ○: 45 Eccentrically-loaded stub columns □: 32 ○: 32 Beam-columns under combined load □: 20 ○: 13 Beam-to-column connection □: 6 ○: 4
Tensile strength of steel σ_u (N/mm^2)	500, 600	400, 600, 800
Compressive strength of concrete F_c (N/mm^2)	26, 44, 62	20, 40, (80), 90
Diameter-thickness ratio	□: 18-56 ○: 15-67	□: 19-74 ○: 17-152
Axial load ratio*1	0.3, 0.5, 0.7	0.2, 0.4, variable*2

*1: ratio to squash load *2: varying between tensile load ratio -0.3 and compressive load ratio 0.7

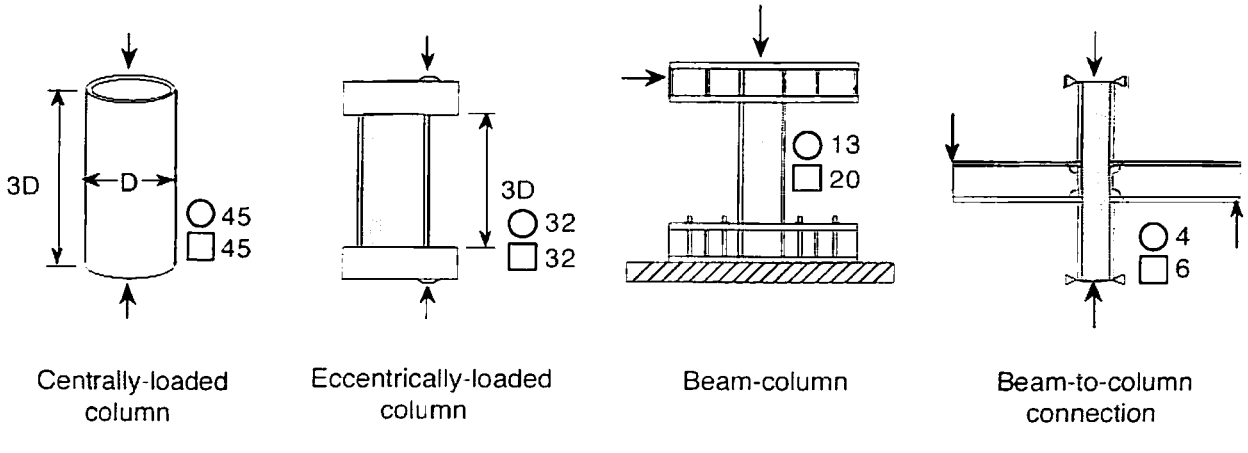

Fig. 4 Tests of CFT Elements

of CFT beam-columns and frames were collected from the Japanese literature published in 1971 through 1995, and a database was developed and maintained. A total of 589 test data (test specimens) were found: 353 beam-columns (242 square and 111 circular) and 236 frames (184 square and 52 circular). Trial designs were carried out for 10-, 24- and 40-story building frames using CFT column system, to look for the merits of employing the CFT system, by comparing constructional costs and structural performance with those of the ordinary steel system. An increase observed in 1995 in Fig. 3 is due to the research related to the U.S.-Japan Program.

In the fifth phase of the U.S.-Japan Cooperative Earthquake Research Program, the CFT investigation produced CFT Guidelines[6]. The Guidelines cover the following topics: i) flow charts for seismic design based on the conventional method using the structural characteristic factor D_S and the performance-based design method which is specified in the recent revision of the Building Standard Law of Japan; ii) constitutive laws for concrete and steel tube derived from the test results of centrally-loaded stub columns, method of analysis for the moment-curvature relation, method of analysis for the load-deformation relation of a beam-column under combined compression, bending and shear, and the model for the restoring-force characteristics of a beam-column which may be used in the analysis of an overall CFT frame; iii) formulas to evaluate stiffness, ultimate strength and deformation capacity of a CFT beam-column, taking into account the confining and scale effects of concrete, the biaxial state of stress and local buckling of the steel tube; iv) the stress transfer mechanism of a beam-to-column connection and a mathematical model for shear force-deformation relation of a connection panel; v) material, manufacturing and fabrication of a steel tube, concrete mixture and casting; vi) design example using an 11-story office building, written for beginners at designing the CFT column system; and vii) investigation of advantages of the CFT column system by the trial design of 10-, 24- and 40-story CFT frames. Some of the research results that formed the background of these Guidelines are summarized in English in BRI Research Paper[7].

3.2 Research Findings

Lessons about the CFT column system learned from the research conducted so far are shown below:

Compression Members

1) The difference between ultimate strength and nominal squash load of a centrally loaded circular CFT short column is provided by the confining effect and estimated by a linear function of the steel tube yield strength[8].

2) For a square CFT short column, strength increase due to the confining effect is much smaller compared to a circular short column. Local buckling significantly affects the strength of a square short column.

3) The buckling strength of a CFT long column can be evaluated by the sum of the tangent modulus strengths calculated for a steel tube long column, and a concrete long column, separately. There is no confinement effect on the buckling strength, regardless of the cross sectional shape[9].

4) Elastic axial stiffness can generally be evaluated by the sum of the stiffness of the steel tube and the concrete. However, careful consideration must be given to the effects of stresses generated in the steel tube at the construction site, the mechanism which transfers beam load to a CFT column through the steel tube skin, and the creep and drying shrinkage of the concrete. These factors may affect the stiffness.

5) Constitutive laws for concrete and steel in a CFT column have been established that take into account the increase in concrete strength due to confinement, the scale effect on concrete strength, the strain softening in concrete, the increase in tensile strength and decrease in compressive strength of the steel tube due to ring tension stress, the local buckling of the steel tube, the effect of concrete restraining the progress of local buckling deformation, and the strain hardening of steel[10].

Beam-Columns

6) The bending strength of a circular CFT beam-column exceeds superposed strength (the sum of the strengths of concrete and steel tube) due to the confinement effect. For a square CFT beam-column, strength increase due to the confining effect is much smaller compared to a circular beam-column. Local buckling significantly affects the strength of a square beam-column.

7) Circular CFT beam-columns show larger ductility than square ones.

8) Use of high strength concrete generally causes the reduction of ductility. However, in the case of a circular CFT

beam-column, non-ductile behavior can be improved by confining concrete with high strength steel tubes.

9) Empirical formulas to estimate the rotation angle limit of a CFT beam-column have been proposed[3].

10) Fiber analysis based on the constitutive laws mentioned above traces the flexural behavior and ultimate strength of an eccentrically loaded CFT column[11].

11) The effective mathematical model has been established to trace the cyclic behavior of a CFT beam-column subjected to combined compression, bending and shear, but not the behavior after the local buckling of the steel tube[12].

12) A hysteretic restoring force characteristic model for a CFT beam-column has been proposed, which accurately predicts the behavior when the rotation angle is less than 1.0%[13].

Beam-to-Column Connections

13) Design formulas have been established for outer and through diaphragms, and the ring stiffener, shown in Fig. 1.

14) Although they are rather complicated, strength evaluation formulas have been proposed for inner diaphragms, which are derived by the yield line theory[3].

15) A stress transfer mechanism has been proposed to trace the load-deformation behavior of a CFT column subassemblage, which consists of a diagonal concrete strut and a surrounding steel frame formed by tube walls and diaphragms[18].

16) Design formulas for the shear panel in the connection have been established, which give the lower bound of the ultimate shear strength.

17) Several new types of connections have been proposed, such as connections using vertical stiffeners[14], long tension bolts[15, 16], and thicker tube at the shear panel without a diaphragm[17].

Frames

18) Tests of subassemblages whose shear panels were designed to be weaker than beams and columns showed very ductile behavior[19]. However, it is usually difficult in practice to make the shear panel weaker unless a steel tube thinner than the CFT column is used for the shear panel.

19) The energy dissipation capacity of a column-failing CFT frame is equivalent to that of a steel frame[20].

Quality of Concrete and Casting

20) As stated above, the bleeding of concrete underneath the diaphragm may produce a gap between concrete and steel. It is necessary to mix concrete with a small water content, a small unit water and a large unit cement to reduce bleeding. Use of superplastisizer is effective to keep good workability[3].

21) The pumping-up method is recommended to cast compact concrete without a void area underneath the diaphragm. Lateral pressure on the steel pipe caused by pumping usually increases to 1.3 times the liquid pressure of concrete (the unit weight of fresh concrete times the casting height), which causes ring tension stress in the steel tube. The pressure and stress may distort the square shape of the tube, if the wall thickness of the tube is too thin[3].

22) When the casting height is not too high, the Tremie tube method is effective with the use of a vibrator to obtain compact concrete. If the vibrator is not used, it is necessary to cast the concrete with high flowability and resistance against segregation.

Design Characteristics

23) The lateral story stiffness of the CFT column system is larger than that of the steel system, but the story weight of the CFT column system is also larger. This leads to no major differences in the vibration characteristics of either system.

24) No significant difference in elasto-plastic behavior or energy dissipation capacity is observed between the CFT and steel systems as long as the overall frame mechanism is designed so that plastic hinges mainly form in the beams[21].

25) Total steel weight of the CFT column system is about 10% less than that of the steel system[21].

Fire Resistance

26) CFT columns elongate at early stage of heat loading, and then shorten until failure.

27) CFT columns can sustain axial load from filled concrete after the capacity of the steel tube is lost by heating, and thus, fireproof material can be reduced or omitted.

28) Rigidity at the beam-to-column connection reduces because of the heat loading, which leads to the reduction of bending moments transferred from beams to columns. Thus, the column carries only axial load at the final stage of heat

loading[22].

24) Fire tests of CFT beam-columns forced to sway by the thermal elongation of adjacent beams have shown that square and circular CFT beam-columns could sustain the axial load for two hours and one hour, respectively, under an axial load ratio of 0.45 and a sway angle of 1/100, but CFT beam-columns could not resist bending caused by the forced sway after 30 minutes of heating[23].

4. CONTRIBUTION OF MIE UNIVERSITY

CFT research in Mie University started in 1990 at the Department of Architecture, and the topics covered and the findings obtained so far are shown below:

Post-Buckling Behavior of Beam-Columns[24, 25] A total of 46 specimens of cantilever beam-columns made of cold-formed square steel tube with or without filled-concrete were tested under a constant axial load and repeated horizontal load, as shown in Fig. 5, in order to clarify the strength deterioration phenomena due to local buckling. The repeated horizontal load was applied at the top of the specimen at a constant displacement, and the effects of the following parameters on the post-buckling behavior of the CFT beam-columns were investigated: existence of filled-concrete, width-to-thickness ratio of steel tube (22, 31 and 43), axial load ratio, which was the ratio of axial load to the squash load of the CFT section (5 to 30 %), and displacement amplitude ratio, which was the ratio of the horizontal displacement amplitude in the repeated horizontal loading to the displacement at the occurrence of the local buckling (0.6 to 1.3). Beam-column behavior was analyzed using a cantilever model shown in Fig. 6(a), based on the assumptions that a uniform bending moment is distributed in the deformable portion, and it obeys the moment-curvature relations calculated from assumed cyclic stress-strain relations of concrete and steel shown in Fig. 6(b). The effect of local buckling of steel tube was considered in the descending portion of the stress-strain relation of steel. Research findings were as follows: i) The horizontal displacement at the occurrence of local buckling became smaller as the axial load ratio increased, but the values of axial strain at local buckling were not much affected by the axial load ratio. ii) The horizontal displacement at the occurrence of local buckling was greater in CFT than in void tube specimens due to the restraining effect of filled-concrete. This delay of local buckling was most pronounced in the specimens with the width-thickness ratio equal to 31. iii) The analysis fairly well traced the experimental behavior, as shown in

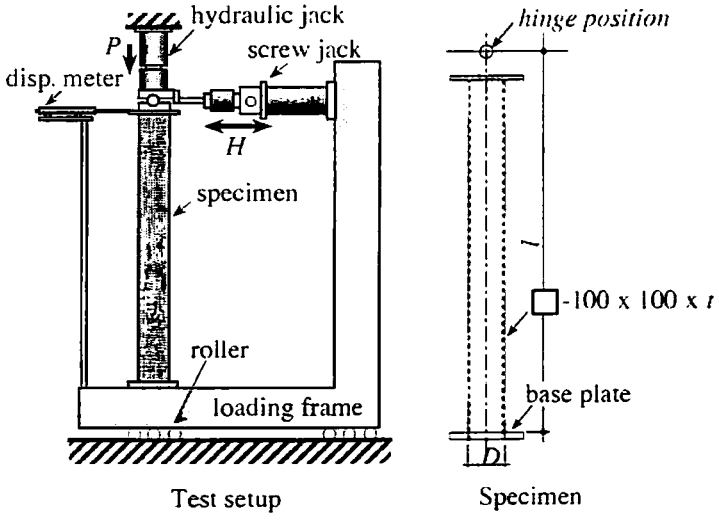

Fig. 5 Test of Beam-Columns

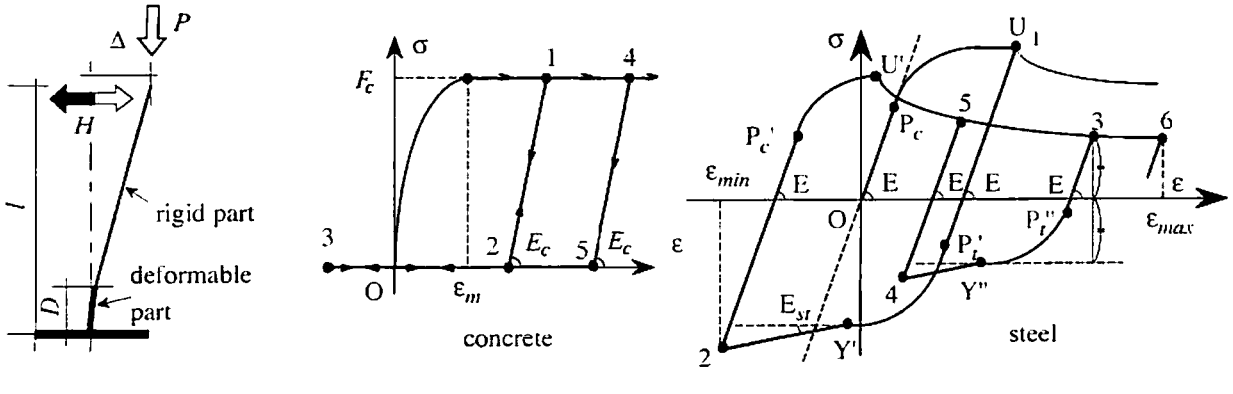

(a) Model of analysis (b) Stress-strain relations

Fig. 6 Analysis of Beam-Columns

Fig. 7. However, the shape of a converged hysteresis loop obtained by the analysis is more like a parallelogram, since Bauschinger's effect is not well traced in the analysis. The $P\delta$ effect is more pronounced in the analysis. iv) The strength deterioration ratio, which is the ratio of the maximum strength observed in the 10th cycle of horizontal loading to that in the first cycle of loading, is illustrated as a membrane in a 3D space in Fig. 8. The ratio became the smallest in the specimens with the width-thickness ratio equal to 31. v) The energy dissipation capacity of CFT specimens was much greater than that of void tube specimens, mainly because the occurrence of local buckling was delayed.

Elasto-Plastic Behavior of Portal Frames[26, 27] A total of 13 specimens of portal frames consisting of square tube columns with or without filled concrete and an H-shaped beam were tested, as shown in Fig. 9, under a constant axial load and repeated horizontal load with increasing displacement amplitude. Test variables were the existence of filled-concrete, the axial load ratio (0.15 and 0.30) and the width-thickness ratio of steel tubes (21, 39 and 54). Figure 10 shows the load-deformation relations of sample specimens. The energy dissipation capacity was mainly investigated, and research findings were as follows: i) All specimens showed fairly stable hysteresis loops, although the local buckling occurred in the steel tubes, except for one of the specimens subjected to the smaller vertical load, in which the fracture occurred in the welded part at the column end, because the fillet welding was accidentally used. ii) In the case of the specimen with the width-thickness ratio equal to 54, the characteristics of concrete were more pronounced, and the hysteresis loops were a little pinched. iii) The strength deterioration occurring after the local buckling was rather large in the case of specimens with the width-thickness ratio equal to 21, since the large percentage of the strength was provided by the steel tube, and the restraining effect of concrete on the growth of the local buckling deformation was

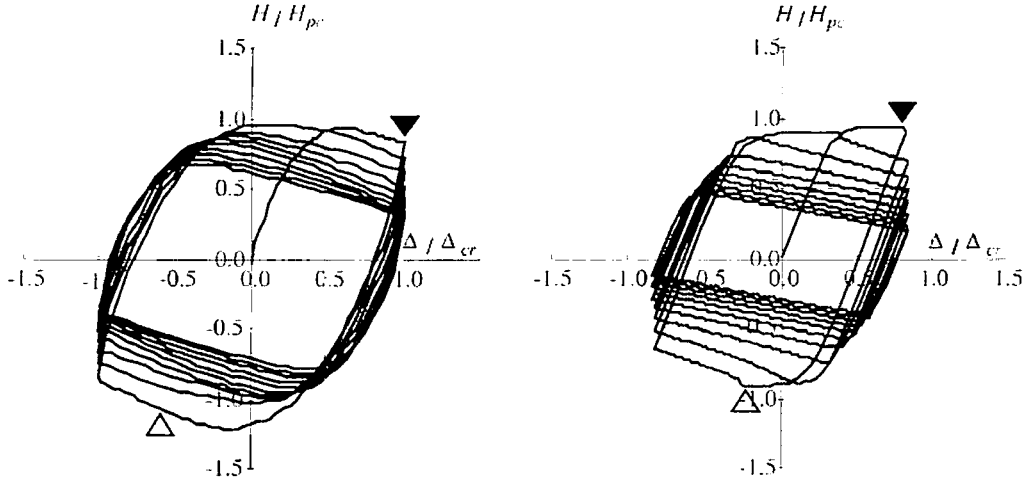

$b/t = 21$ $n = 0.15$ displacement amplitude ratio = 1.0

Fig. 7 Load-Displacement Relations of Beam-Columns

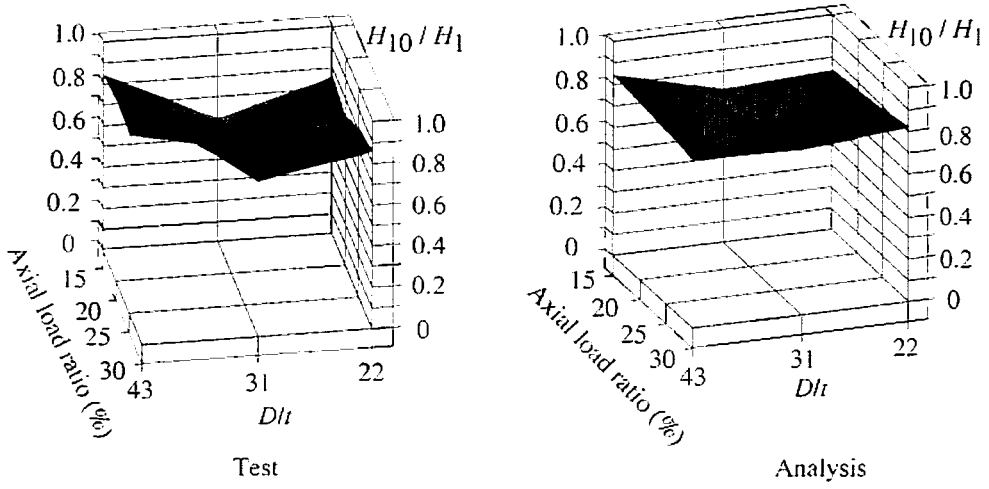

Fig. 8 Strength Deterioration Surface

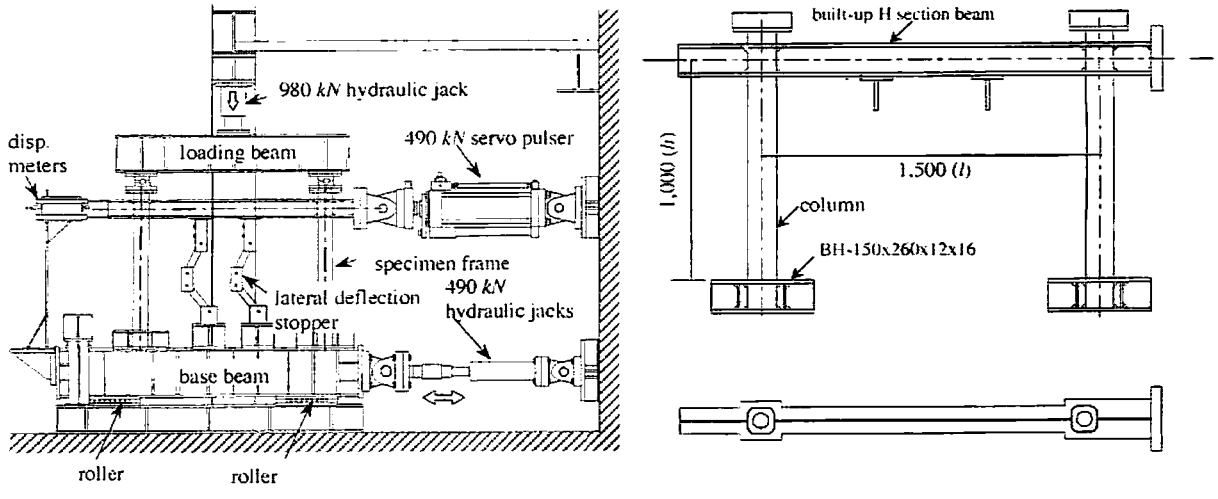

Test setup Specimen

Fig. 9 Test of Portal Frames

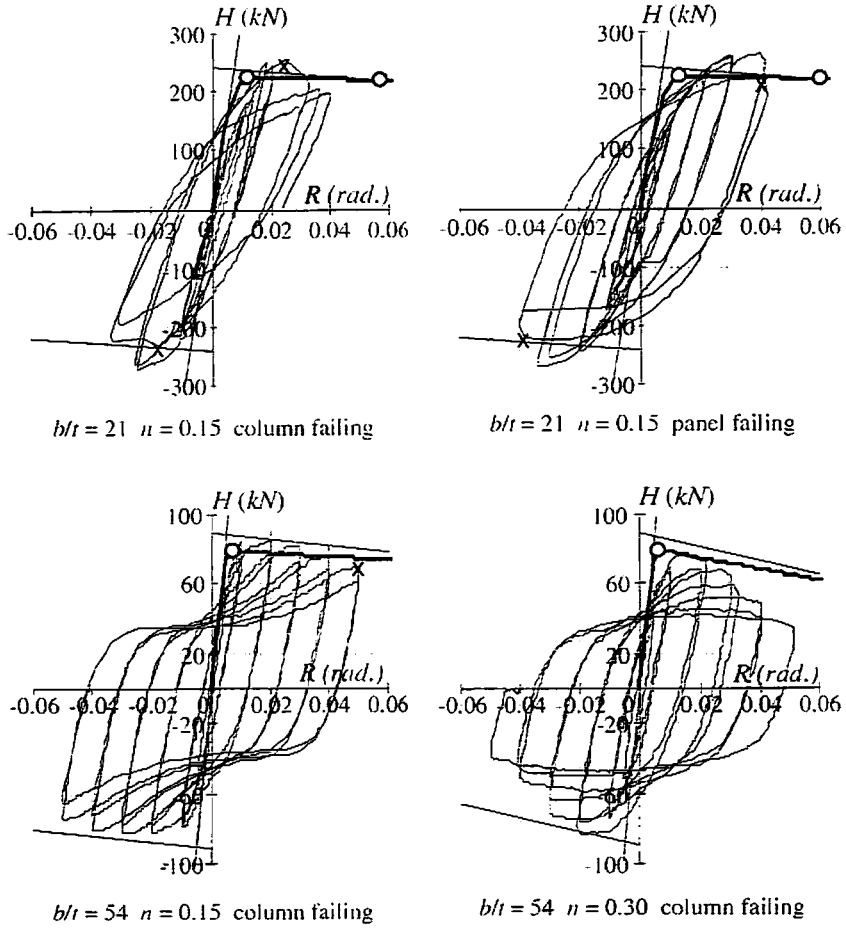

Fig. 10 Load-Displacement Relations of Portal Frames

not much expected. On the other hand, in the case of specimens with the width-thickness ratio equal to 54, the strength deterioration was small since the concrete restraining was effective. iv) The values of the structural characteristic factor D_s obtained from the tests data, which is an index of the energy dissipation capacity, highly depended on the loading history and the number of loading cycles. Those obtained from the cumulative plastic deformation capacity were quite smaller than the values used in the real design practice of pure steel frames, and the maximum difference was observed in the specimens with the width-thickness ratio equal to 39, as shown in Fig. 11.

Elasto-Plastic Behavior of Three-Dimensional Frames[28, 29] A total of 18 3D- and 4 2D- frame specimens consisting

of square CFT columns and H-shaped beams were tested, as shown in Fig. 12, under a constant axial load on the column, constant beam loads in the minor direction, and alternately repeated beam shear in the major direction simulating the earthquake loading. Figure 13 shows the loading patterns. Test variables were as follows: shapes of specimen (interior, exterior, and corner column types); failure types (panel failing, and column failing types); and pattern of the long-term loads on the beams in the minor direction ($W_1 = W_2$, $W_1 > W_2$, and $W_2 = 0$), and the axial load ratio (15 and 30 %). Figure 14 shows the load-deformation relations of sample specimens. Research findings were as follows: i) The effects of neither the three-dimensional loading nor the biaxial bending on the maximum strengths were observed in all specimens. ii) Strength deterioration due to cyclic loading was observed in column failing specimens, while little deterioration was observed in connection failing specimens. iii) Beam-to-column connection panels of panel failing specimens yielded and deformed by shear, but the strength increased after the panel yielded, and the plastic hinge formed in the column, except for the planar specimen. This increase is due to the confinement of concrete and strain hardening of steel. In the case of the planar specimen, this increase was not enough, and thus the column remained elastic. iv) Panel failing frames are more advantageous than column failing frames in view of the deformation capacities. v) Axial load reduced the deformation capacity, regardless of the failing types. vi) Two types of the failure modes were observed in three-dimensional specimens. All specimens subjected to the biaxial bending in columns showed the doglegged deformation of the column, and failed with the excessive displacement at the connection. Panel failing specimens subjected to the uni-axial bending showed stable symmetrical deformation and could sustain the axial load until the end of the test.

Strength and Stiffness of CFT Semi-Embedded Column Bases[30, 31] Monotonic and cyclic loading tests were carried

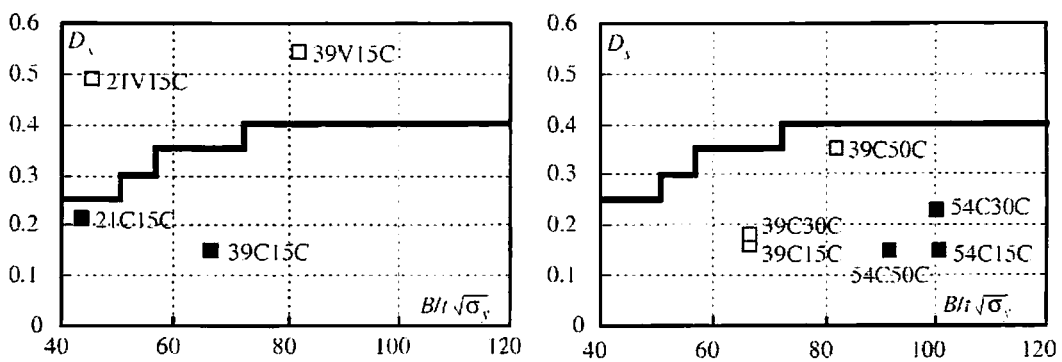

effect of filled-concrete effect of axial load

Fig. 11 D_s Factor

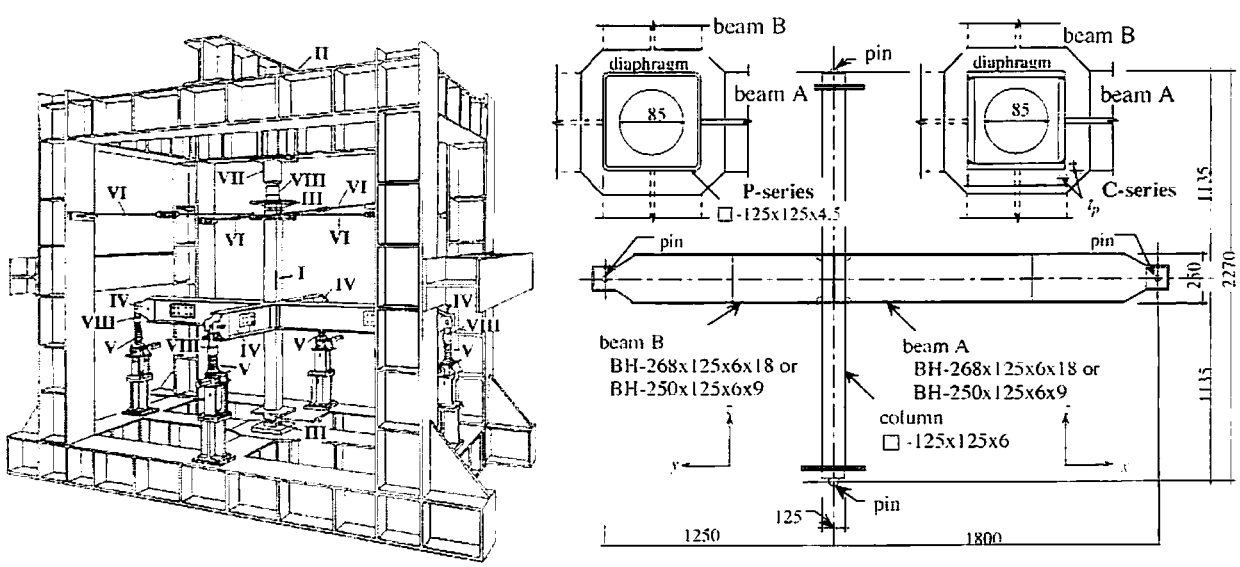

Test setup Specimen

Fig. 12 Test of 3D Frames

out, in order to clarify strength and stiffness of a CFT semi-embedded column base shown in Fig. 15, which was newly developed to improve the performance of a conventional bare type column base. 2 groups of 4 specimens with different embedded lengths were tested under monotonic and cyclic horizontal load. Figure 16 shows the test setup and the detail of specimen. The strength was evaluated, considering three kinds of resisting action; anchor bolt-base plate action,

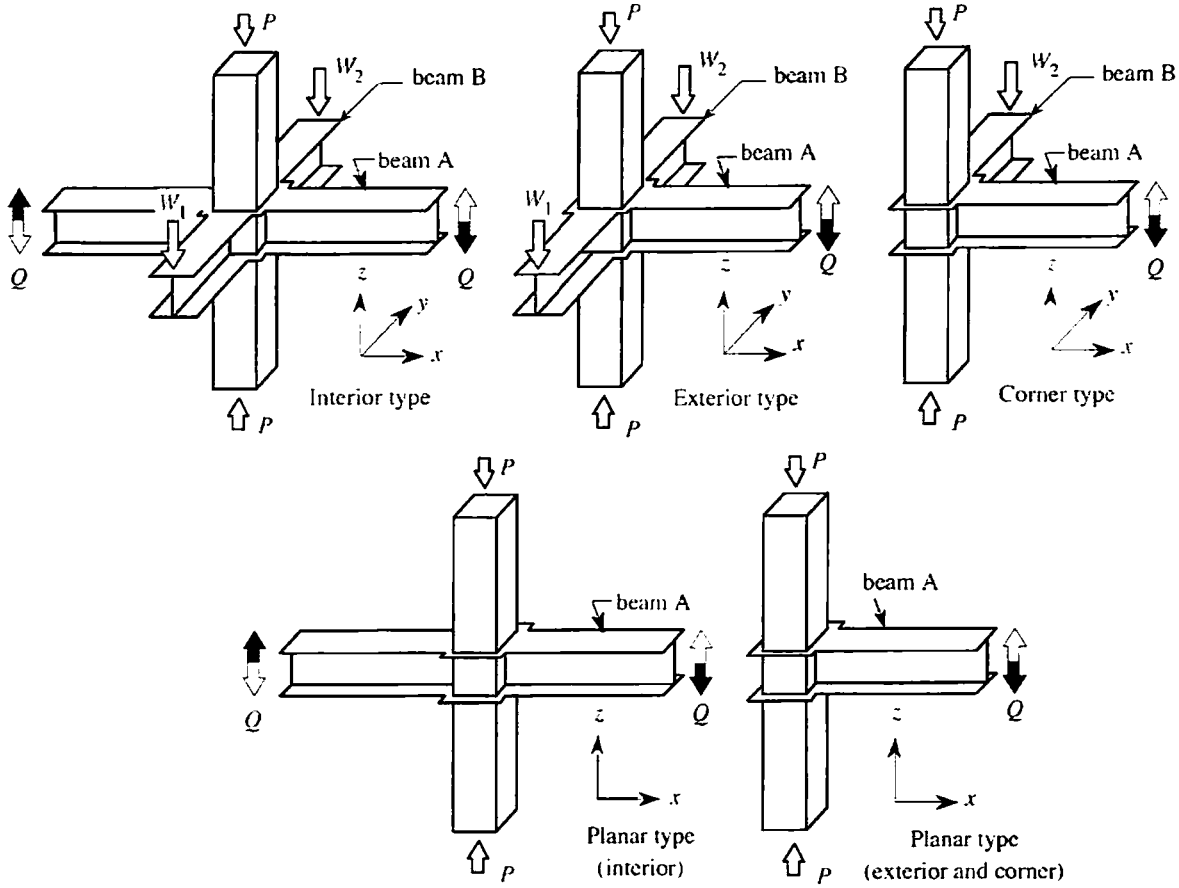

Fig. 13 Loading Pattern

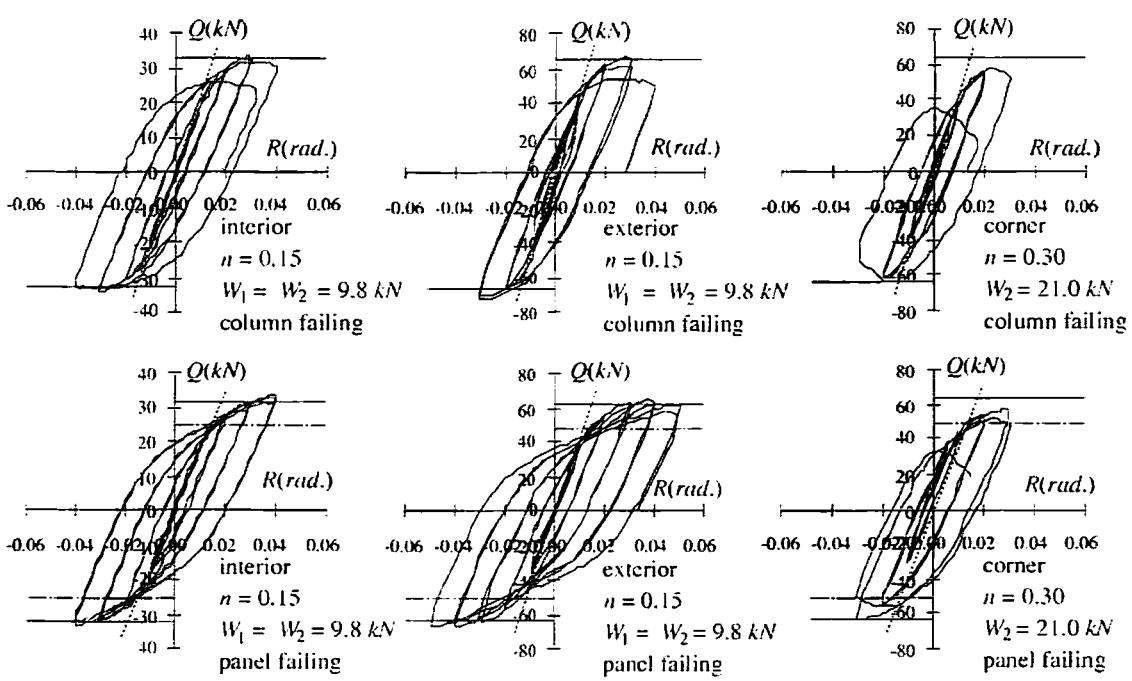

Fig. 14 Load-Deformation Relations of 3D Frames

prying action of the embedded portion of the CFT column, and tension of vertical reinforcing bars in the foundation. Methods to evaluate the strength and stiffness of the specimens were proposed. The hysteresis loops are shown in Fig. 17, together with the calculated strength and stiffness. Research findings were as follows: i) The hysteresis loops of specimens with longer embedded length showed the stable spindle shape, but those with shorter length showed the pinched shape. ii) The maximum strengths of specimens were fairly well estimated by the ultimate strength calculated considering three resisting mechanisms; a) prying action of the embedded portion of the column, b) combined action of the anchor bolts, the base plate and the concrete beneath the base plate, and c) resistance by the anchor plate and the vertical reinforcing bars. iii) It has been tried to estimate the initial stiffness of the specimens by two models: the one mainly considered the deformations of anchor bolts, base plate, and concrete beneath the base plate, and the other mainly considered the deformations of the embedded portion of the column and concrete caused by the prying action. However, the estimation method needs refinement, and more rigorous method should be established.

Creep of CFT Members and Buckling Strength Affected by Creep[32, 33] Fundamental study on the creep of concrete in a CFT member was carried out conducting the creep tests of 6 centrally and 2 eccentrically loaded compression members, and a beam. Figure 18 shows a test setup for the compression member, and the time history of the load carried by concrete and steel calculated from the data of longitudinal strain detected by the wire strain gauges

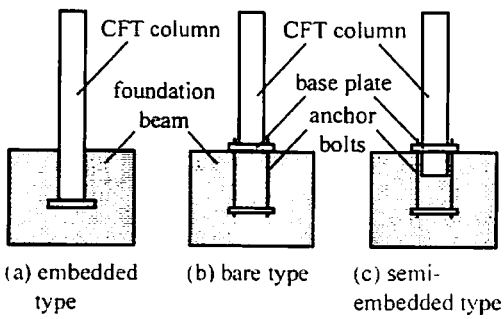

Fig. 15 Column Base Configurations

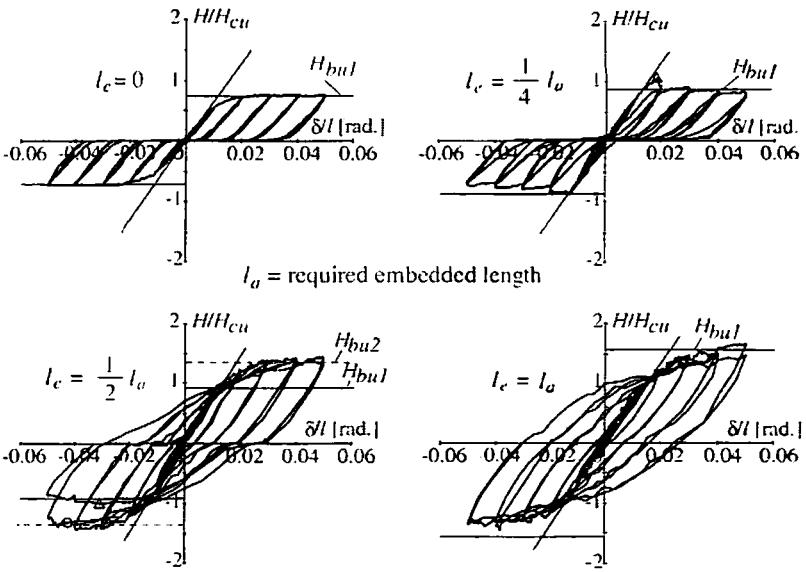

Fig. 17 Load-Deformation Relations

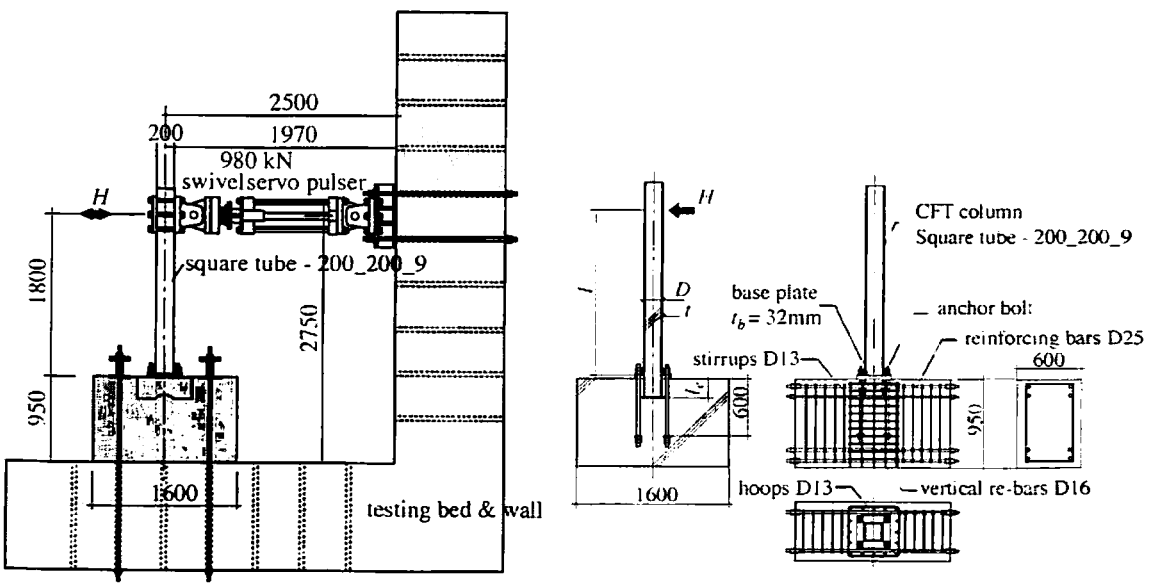

Fig. 16 Test of Semi-Embedded Column Base

mounted on the steel tube surface. It is observed that the load on steel gradually increased because of the creep of concrete. The time history data of creep coefficient ϕ and reduction factor ξ of the elastic modulus of concrete obtained from the beam-column tests are shown in Fig. 19. Based on these data for the creep characteristics of CFT members, the effects of creep on the buckling strength of CFT compression members were theoretically investigated. Research findings were as follows: i) The effect of the specimen length on the creep behavior is not clear, and left for the future investigation. ii) The time-history of creep strain can be traced by the analysis based on the visco-elastic model. iii) The values of the creep coefficient ϕ and the reduction factor of elastic modulus of concrete ξ of CFT members are much smaller than the values indicated for the ordinary reinforced concrete members. iv) The values of ϕ and ξ seem to depend upon the loading conditions. The maximum values were obtained from the centrally loaded compression specimens, and the minimum from the beam specimen. The values of the eccentrically-loaded compression specimens were in between. v) The buckling strength calculated on the assumption that the buckling occurs t days after the application of the load does not vary much if the day t is set more than 50 days. vi) The amount of axial stress carried by the steel tube does not vary much regardless of the day of the buckling occurrence.

Size Effect on Ultimate Strength of CFT Short Columns[34-36] Compression tests of concrete-filled steel tube (CFT) short columns have been conducted to clarify the scale effect on the compression behavior of CFT short columns. The experimental variables were as follows: shape of tube (circular and square), size of specimen (100, 200, 300 and 400mm), strength of filled-concrete (27, 36, 48 and 66 N/mm^2), width-thickness ratio (31, 44 and 50), and loading method (applying the compression load only on the filled-concrete and on the overall cross-section). Figure 20 shows the values of the maximum strength obtained in the tests divided by the calculated ultimate strength against the values of the tube size. The size effect on th strength of circular specimens is not clear, while that on the strength of square specimens is quite clear as shown in (a), and the maximum strength is fairly accurately evaluated by the calculation considering the size effect, as shown in (b). Figure 21 shows the data of 199 circular and 224 square specimens collected from the published literatures, from which it is observed that the evaluation of the maximum strength is fairly good. Research findings were as follows: i) Size effect in the circular CFT specimens does not clearly appear, since it is hidden in the strength increase due to the confining effect. ii) Size effect in the square CFT specimens appears clearly, since the confining effect is small. iii) Confining effect on the concrete strength was also observed in square CFT short columns. iv) Newly-proposed formula for the ultimate strength shows a fairly good evaluation to the experimental values.

Database of CFT Beam-Columns and Frames[37] Test data of CFT beam-columns and frames were collected from the Japanese literatures, and a database mentioned in the Sect. 3.1.3 was developed and maintained as a part of

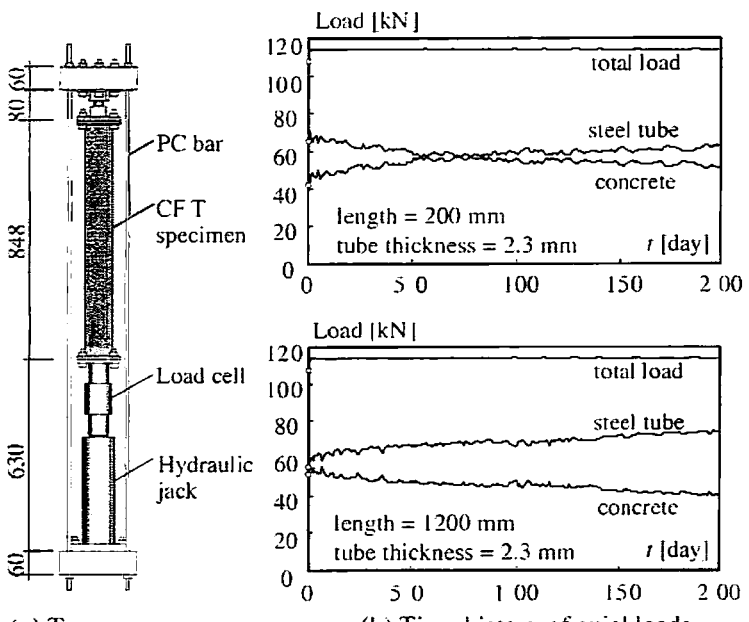

(a) Test setup

(b) Time history of axial loads carried by components

Fig. 18 Creep Tests of Centrally Loaded CFT Compression Members

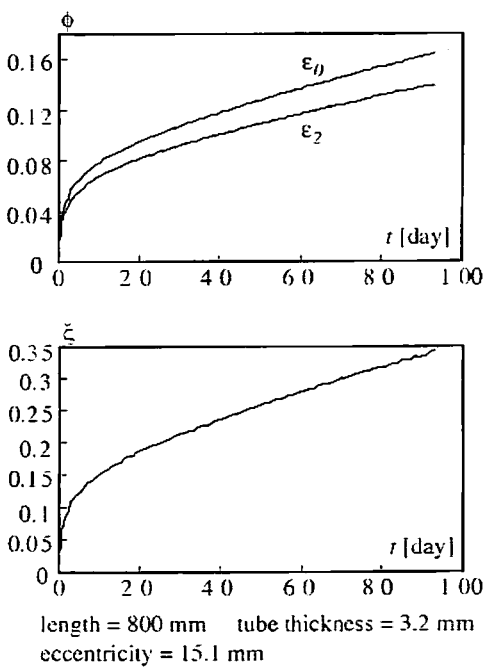

length = 800 mm tube thickness = 3.2 mm
eccentricity = 15.1 mm

Fig. 19 Creep Coeficient ϕ and Reduction Factor of Elastic Modulus ξ of Eccentrically Loaded Columns

the U.S.-Japan Cooperative Earthquake Research Program. The database contains the data concerning the following parameters: loading condition, material properties of concrete and steel tube, shapes and dimensions of the specimen, loads at important events, such as at the maximum point and at the chord rotation angle reaching 1/100, rotation angles at important events, such as at the maximum load and at the load reduced to 95% of the maximum load, and secant stiffness. The ultimate strength and the elastic stiffness are calculated and contained in the database. A multi-linear model of restoring force characteristics of a CFT beam-column is constructed from the database, that is, the relation between the moment M and chord rotation angle R, as shown in Fig. 22, in which the elastic stiffness K_e and the ultimate moment M_{ul} are calculated values, and the values of rotation angles at points B, C and D were obtained by the regression analysis of the test data. Figure 23 compares the model(solid line) and the test results(dashed line) for selected specimens. Research findings were as follows: i) The ultimate bending strength based on the full plastic state of stress considering the interaction between steel tube and concrete gives the lower bound strength of CFT beam-columns with moment gradient. The strength obtained in the tests was much larger than the calculated ultimate strength, mainly

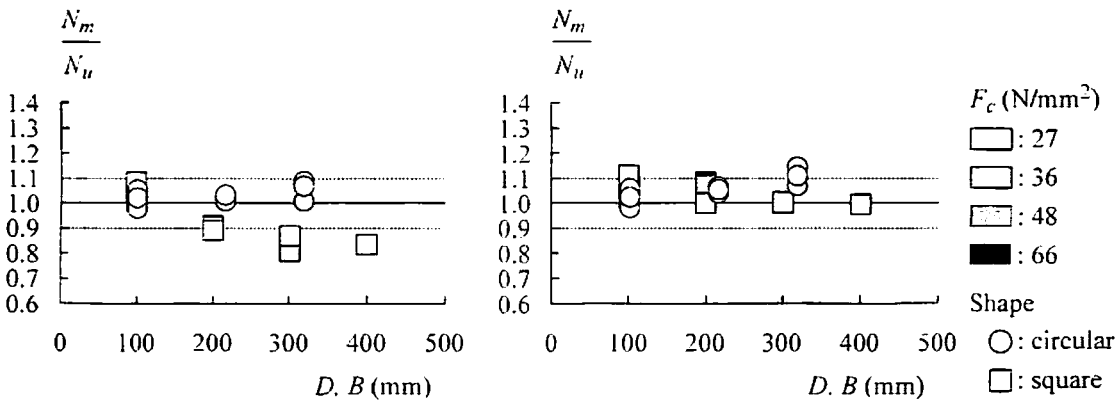

(a) size effect not considered (b) size effect considered

Fig. 20 Size Effect on Ultimate Strength

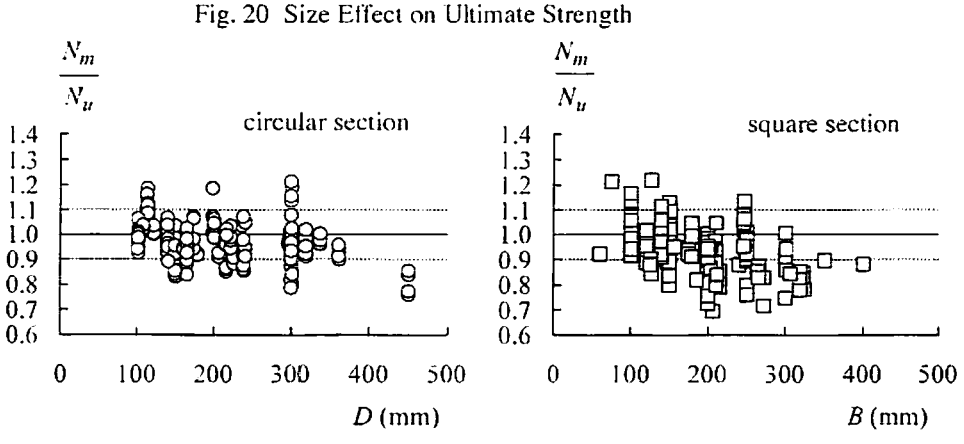

(a) size effect not considered

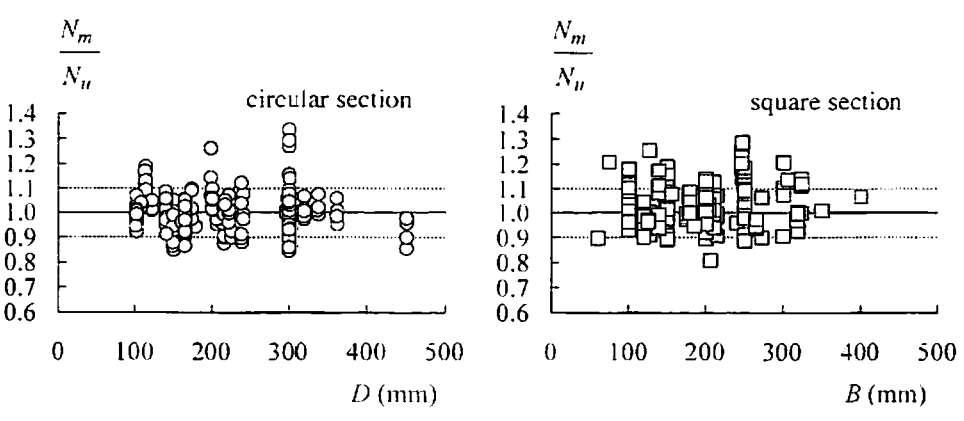

(b) size effect considered

Fig. 21 Evaluation of Compressive Strength of CFT Short Columns

because of the strain hardening and the shift of critical section inside from the end of specimen. ii) Prediction formulas for the rotation capacity give the average value of the capacity obtained in the tests of square CFT specimens, and the lower bound in the case of circular CFT specimens. iii) The multi-linear model proposed here for the restoring-force characteristics of CFT beam-columns shows fairly good agreement with the tests data. This model may be used in the pushover analysis of the frames consisting of CFT columns.

Analysis of 3D CFT Frames[38, 39] A procedure of the elasto-plastic analysis of 3D frames consisting of CFT columns and H-shaped steel beams were proposed. The effects of biaxial bending, local buckling and strain hardening were considered in the analysis of the column. A mathematical model to analyze the relation between the shear force and the shear deformation of a CFT shear panel at the beam-to-column connection consists of elastic-perfectly plastic steel panels, and a number of concrete plates forming after the shear cracks occur, which resist the shear force by diagonal compression forces, as shown in Fig. 24. Load-deformation relations of the columns, beams and shear panel calculated separately were superposed to obtain the deformation of the total system. Figure 25 compares the results of analysis and the tests of column or panel failing planer and 3D CFT subassemblages. Research findings were as follows: i) When the same size of steel tube was used for the column and the shear

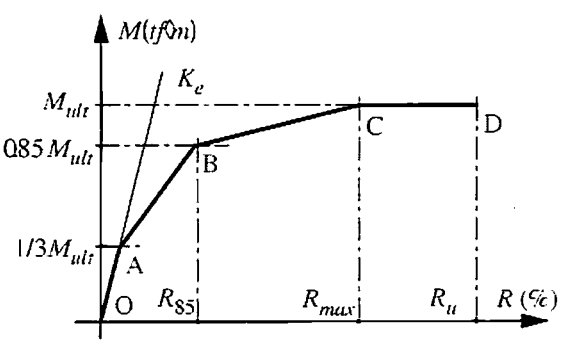

Fig. 22 Model of Restoring-Force Characteristics

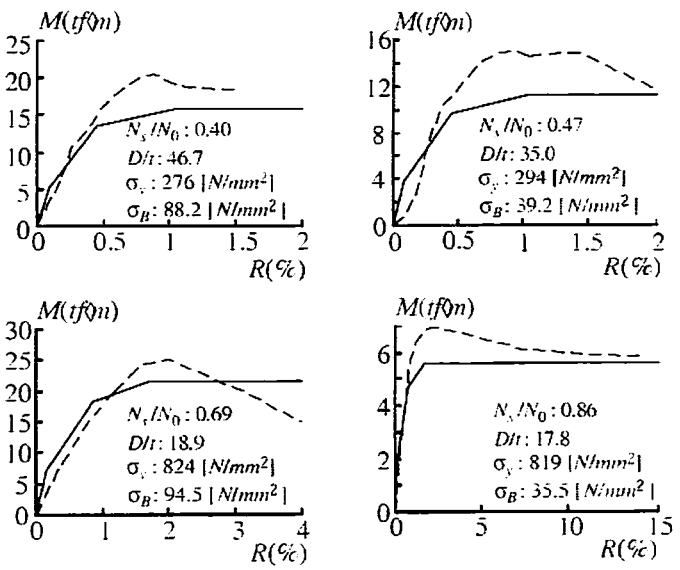

Fig. 23 Comparison of Restoring-Force Characteristics

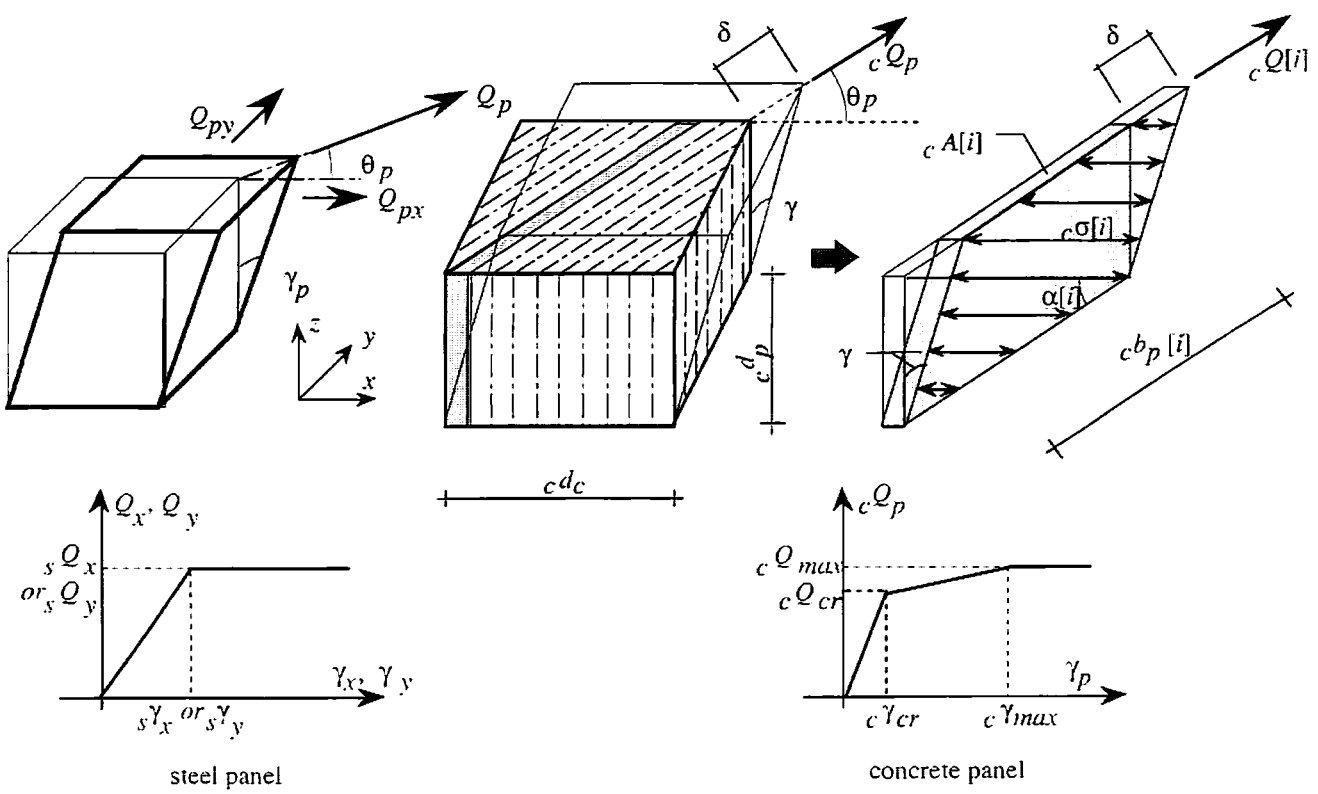

Fig. 24 Model of Connection Panel

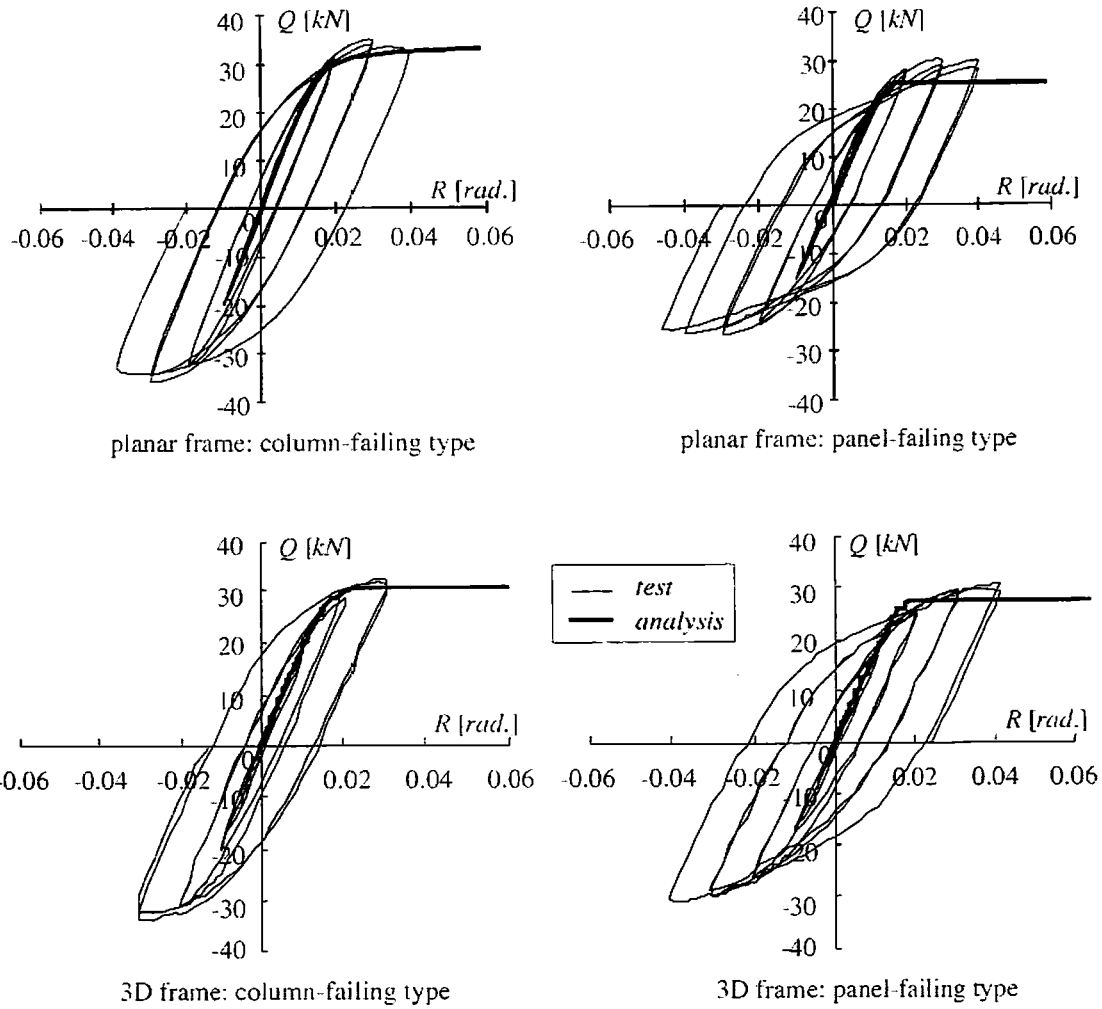

Fig. 25 Comparison of the Results of Test and Analysis

panel, the steel frame tended to yield in the shear panel first, while that of CFT tended to yield in the column first. ii) The most effective factors to affect the strength ratio of column against the connection are the volume of the connection zone and the strength of filled-concrete. iii) The maximum strength of the column yielding specimens was well predicted by the analysis, which included the effects of the strain-hardening, the local buckling of the steel tube and the confinement of concrete. On the other hand, the maximum strength of the panel failing specimens exceeds the strength obtained from the analysis, mainly because the effect of the strain-hardening was not included when evaluating the shear strength of the steel panel.

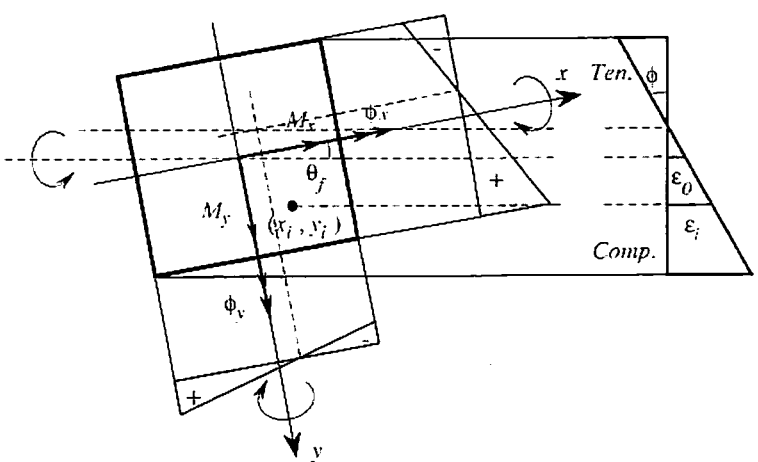

Fig. 26 Section under Biaxial Bending

Biaxial Bending Behavior of Steel-Concrete Composite Sections[40, 41] Effects of loading path on the ultimate strength and the moment-curvature relation of composite cross sections subjected to axial load and biaxial bending were investigated by analyzing four kinds of cross section: steel wide-width H-shape, steel square tube, concrete-filled steel square tube and SRC containing steel wide-width H-shape. Three types of loading path were considered, referring to the

section subjected to biaxial bending shown in Fig. 26: A) monotonically increasing bending moment M_x with constant M_y, B) proportional deformation with a constant ratio of biaxial curvatures ϕ_y/ϕ_x, and C) proportional loading with a constant ratio of bending moments M_y/M_x. Figures 27 and 28 show M_x-M_y paths with the ultimate strength interaction curves, and the moment curvature relations, respectively, both calculated for the hollow steel tube and CFT sections. Research findings were as follows: i) An identical point on the interaction curve for the ultimate strength of the cross section subjected to the axial load and the biaxial bending moment was reached regardless of the loading procedure. ii) The moment-curvature curves obtained from three different analyses met at one point, and the values of the moments at this point are on the interaction curve for the ultimate strength. iii) The ultimate strength point on the interaction curve was not the same as the maximum strength point of M_x and M_y in the case of the procedure B for the section having unequal strengths about two major axes.

Analysis of Beam-Columns Having Unstable Stress-Stain Relation[42, 43]

Elasto-plastic and post-buckling analysis was performed to solve the deflections of a beam-column which was made of a material having the unstable stress-stain relation. A mathematical model considered was the cantilever column subjected to a constant vertical and increasing horizontal loads, as shown in Fig. 29(a). In the conventional analysis procedure, the column is first divided into small elements along the longitudinal axis, and the deflection is computed by numerical integration of the curvature, which is assumed to be uniformly distributed

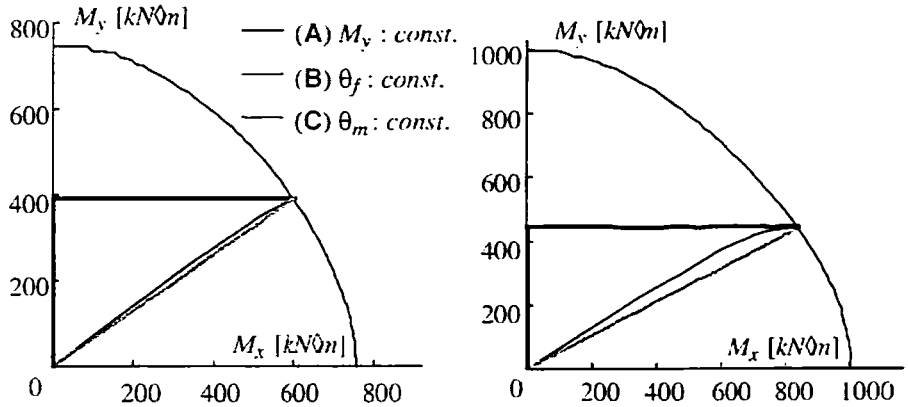

(a) Square hollow section (b) CFT

Fig. 27 Ultimate Strength for Biaxial Bending

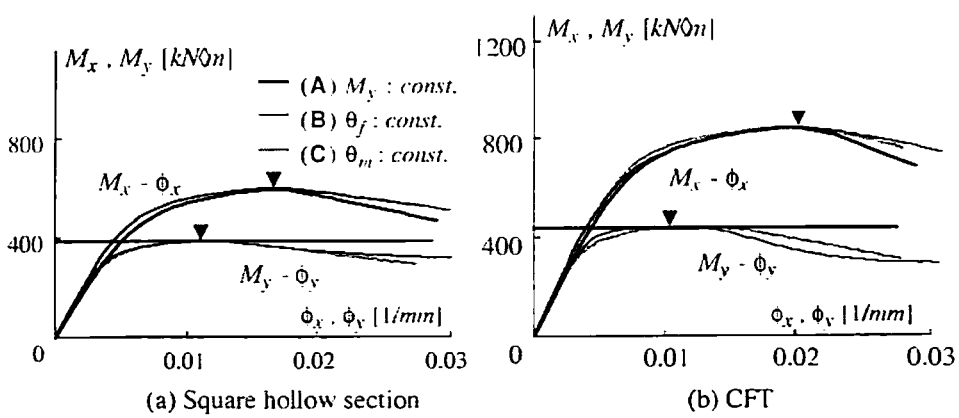

(a) Square hollow section (b) CFT

Fig. 28 Moment-Curvature Relations

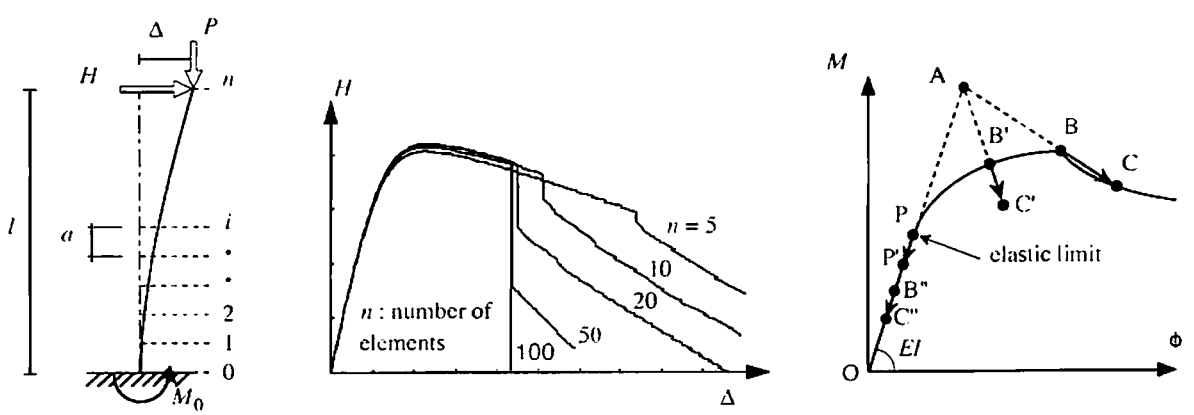

(a) Model (b) H-Δ relations (c) Moment-curvature path

Fig. 29 Model for the Analysis of Beam-Column Behavior

in each element. However, this procedure is not applicable to the column having an unstable moment-curvature relation: the solution for the load-displacement relation depends upon the number of elements, as shown in Fig. 29(b), and a unique solution cannot be obtained. A new method was proposed, in which the solution satisfying the equilibrium at each subdivision point was searched by a proposed way of combining the degrading type moment-curvature relation with the numerical integration scheme. It was assumed that as the M-ϕ point of the critical element (the first element at the base) moves from the point B to C in Fig. 29(c), the M-ϕpoints in other inelastic elements move from the point B' to C', and that in elastic elements from the point B" to C", and so forth, on the lines connecting the points A and B' or B", respectively. This idea was extended to the cyclic moment curvature relations, and applied to the analysis of hollow steel tube and CFT beam-columns failing in the local buckling of the steel tube. Figure 30 compares the results of test and analysis. Research findings were as follows: i) The solution obtained from the proposed method of analysis was independent of the number of subdivided elements. ii) The analysis well traced the characteristics of the test results, such as the local buckling, the strength deterioration due to cyclic loading, the pinching of hysteresis loops due to concrete cracks, and the convergence-divergence of the hysteresis loops.

5. DESIGN PROVISIONS FOR CFT COLUMN SYSTEM

The newest edition of SRC Standards of AIJ was published in 2001[2], based on the CFT Recommendations[3], as mentioned before. This section introduces the provisions for the design of CFT columns and beam-to-column connections, specified in SRC Standards of AIJ[2].

i) Ultimate Compressive Strength of a CFT Column

Ultimate compressive strength of a CFT column is calculated by Eqs. (1) ~ (4).

$\frac{l_k}{D} \leq 4$: $N_{u1} = N_u^c + (1+\eta) N_u^s$ (1)

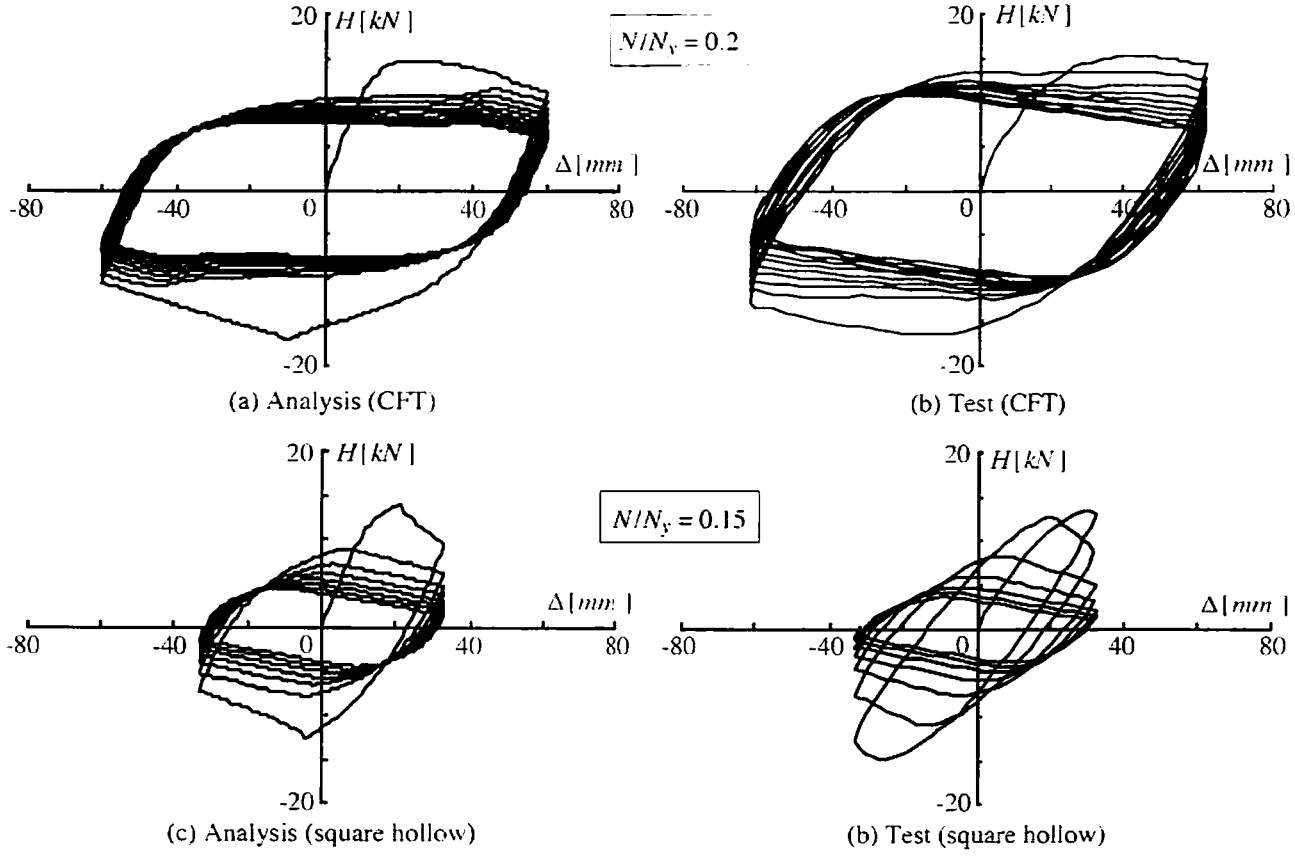

(a) Analysis (CFT) (b) Test (CFT)

(c) Analysis (square hollow) (b) Test (square hollow)

Fig. 30 Comparison of Load-Deflection Relations

$$12 < \frac{l_k}{D} \qquad N_{u3} = N_{cr}^{c} + N_{cr}^{s} \tag{3}$$

where

l_k : effective length of a CFT column

D : width or diameter of a steel tube section

$$\eta = 0 \text{ for a square CFT column} \qquad \eta = 0.27 \text{ for a circular CFT columr} \tag{4}$$

N_{u1} , N_{u2} , N_{u3} : ultimate strength of a CFT column

N_{u}^{c} : ultimate strength of a concrete column

N_{u}^{s} : ultimate strength of a steel tube column

N_{cr}^{c} : buckling strength of a concrete column

N_{cr}^{s} : bucklin strength of a steel tube column

N_{u1} in Eq. (1) gives cross-sectional strength of a CFT column, in which strength of confined concrete is considered for circular CFT. Derivation of $\eta = 0.27$ is shown in Ref. [8]. N_{u3} in Eq. (3) gives buckling strength of a long column as the sum of the buckling strengths separately computed for filled-concrete and steel tube long columns. Accuracy of Eq. (3) compared with the tangent modulus load of CFT columns is discussed in Ref. [9].

Ultimate compressive strength N^{c}_{u} and buckling strength of N^{c}_{cr} of filled concrete column are calculated by Eqs. (5) and (6).

$$N_{u}^{c} = A_c \, r_u \, F_c \tag{5}$$

$$N_{cr}^{c} = A_c \, \sigma_{cr}^{c} \tag{6}$$

where

A_c : cross-sectional area of a concrete column

F_c : design standard strength of filled concrete

σ_{cr}^{c} : critical stress of a concrete column

$r_u = 0.85$: reduction factor for concrete strength

Critical stress σ^{c}_{cr} is given by Eqs. (7) ~ (10).

$$\bar{\lambda}_c \le 1.0; \qquad \sigma_{cr}^{c} = \frac{2}{1 + \sqrt{\bar{\lambda}_c^{4} + 1}} \, r_u \, F_c \tag{7}$$

$$1.0 < \bar{\lambda}_c; \qquad \sigma_{cr}^{c} = 0.83 \, exp \{ C_c (1 - \bar{\lambda}_c) \} \, r_u \, F_c \tag{8}$$

where

$$\bar{\lambda}_c = \frac{\lambda_c}{\pi} \sqrt{\varepsilon_u^{c}} \tag{9}$$

$$\varepsilon_u^{c} = 0.93 \, (r_u \, F_c)^{\frac{1}{4}} \times 10^{-3} \tag{10}$$

$$C_c = 0.568 + 0.00612 \, F_c \tag{11}$$

λ_c : slenderness ratio of a concrete column

In Eqs. (10) and (11), the value of F_c should be given in N/mm^2. Equations (7) and (9) are obtained by curve fitting

numerical results of tangent modulus load of long concrete columns. Strength increase of confined concrete is not considered. Details are shown in Ref. [9].

Ultimate compressive strength N^s_u of steel tube column is calculated by Eq. (12).

$$N^s_u = A_s F_s \tag{12}$$

where

A_s : cross-sectional area of a steel tube column

F_s : design standard strength of steel tube

Buckling strength of N^s_{cr} of steel tube column is calculated by Eqs. (13) and (17).

$$\bar{\lambda}_s \le 0.3 ; \qquad N^s_{cr} = A_s F_s \tag{13}$$

$$0.3 \le \bar{\lambda}_s < 1.3 ; \quad N^s_{cr} = \{ 1 - 0.545 (\bar{\lambda}_s - 0.3) \} A_s F_s \tag{14}$$

$$1.3 \le \bar{\lambda}_s : \qquad N^s_{cr} = \frac{N^s_E}{1.3} \tag{15}$$

where

$$\bar{\lambda}_s = \frac{\lambda_s}{\pi} \sqrt{\frac{F_s}{E_s}} \tag{16}$$

$$N^s_E = \frac{\pi^2 E_s I_s}{l_k^2} \tag{17}$$

λ_s : slenderness ratio of a steel tube column

E_s : Young's modulus of steel tube

I_s : cross-sectional moment of inertia of a steel tube column

Equations (13) ~ (15) are expressions of the column curves used in Japan for the plastic design of steel structures[44].

ii) Ultimate Bending Strength of a CFT Beam-Column

Ultimate bending strength M_u of a CFT beam-column subjected to axial load N is calculated by the following procedure. First, M_u of a beam-column not longer than 12 times width or diameter of steel tube is calculated by Eqs. (18) and (19).

$$N = N^c_u + N^s_u \tag{18}$$

$$M_u = M^c_u + M^s_u \tag{19}$$

The strengths appearing on the right hand side of Eqs. (18) and (19) are given as follows:
For rectangular CFT:

$$N^c_u = \bar{x}_n D_c^2 r_u F_c \tag{20}$$

$$M^c_u = \frac{1}{2} (1 - \bar{x}_n) \bar{x}_n D_c^3 r_u F_c \tag{21}$$

$$N^s_u = 2 (2 \bar{x}_n - 1) D_c^2 t F_s \tag{22}$$

$$M^s_u = \{ (1 - \frac{t}{D}) D^2 + 2 (1 - \bar{x}_n) \bar{x}_n D_c^2 \} t F_s \tag{23}$$

For circular CFT:

For circular CFT:

$$N_u^c = \frac{1}{4}(\theta_n - \sin\theta_n \cos\theta_n) D_c^2 \sigma'_B \tag{24}$$

$$M_u^c = \frac{1}{12}\sin^3\theta_n D_c^3 \sigma'_B \tag{25}$$

$$N_u^s = \{\beta_1 \theta_n + \beta_2(\theta_n - \pi)\}(1 - \frac{t}{D}) D t F_s \tag{26}$$

$$M_u^s = \frac{1}{2}(\beta_1 + \beta_2)\sin\theta_n (1 - \frac{t}{D})^2 D^2 t F_s \tag{27}$$

where

$$\bar{x}_n = \frac{x_n}{D_c} \tag{28}$$

$$\theta_n = \cos^{-1}(1 - 2\bar{x}_n) \tag{29}$$

$$\sigma'_B = r_u F_c + \frac{1.56 t F_s}{D - 2t} \tag{30}$$

$$\beta_1 = 0.89, \qquad \beta_2 = 1.08 \tag{31}$$

D_c : width or diameter of a concrete section

t : thickness of a steel tube section

x_n : position parameter of neutral axis

The equilibrium conditions between internal and external forces are given by Eqs. (18) and (19), and axial and bending strengths carried by concrete and steel tube at the ultimate state are calculated by Eqs. (20) ~ (31), based on the stress distributions shown in Fig. 31 with the neutral axis at the distance x_n from the extreme compression fiber. The P δ effect is not considered, and thus they are the cross-sectional strengths. The strength increase of confined concrete is considered in σ'_B, and the changes in axial compressive and tensile yield stresses of steel tube due to ring tension are considered by β_1 and β_2, respectively[8].

M_u of a CFT beam-column longer than 12 times width or diameter of steel tube is calculated by Eqs. (32) and (33).

$$N \le N_{cr}^c; \qquad M_u = \frac{1}{C_M}\{\bar{M}_u^c + M_p(1 - \frac{N}{N_k})\} \tag{32}$$

$$N > N_{cr}^c; \qquad M_u = \frac{1}{C_M}\bar{M}_u^s(1 - \frac{N_{cr}^c}{N_k}) \tag{33}$$

where

$$\bar{M}_u^c = \frac{4N}{0.9 N_{cr}^c}(1 - \frac{N}{0.9 N_{cr}^c})\frac{C_b}{C_b + \bar{\lambda}_c^2} M_0^c \tag{34}$$

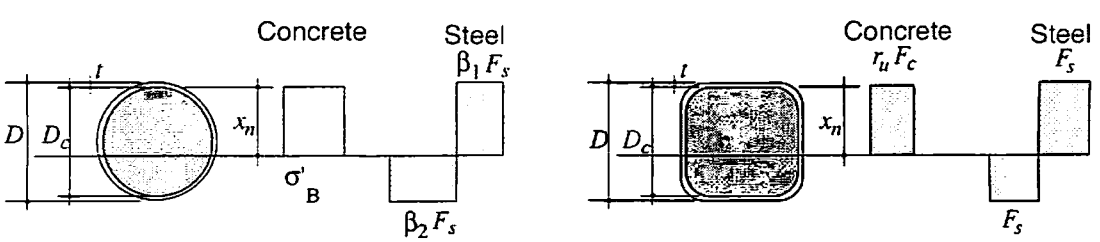

Fig. 31 Stress Blocks for Ultimate Bending Strength

$$M_0^c = \frac{r_u F_c D^3}{8} \quad \text{for a square CFT beam-column}$$
$$M_0^c = \frac{r_u F_c D^3}{12} \quad \text{for a circular CFT beam-column} \tag{35}$$

$$\frac{N - N_{cr}^c}{N_{cr}^s} + \frac{\bar{M}_u^s}{(1 - \frac{N - N_{cr}^c}{N_E^s}) M_p} = 1 \tag{36}$$

M_p : full plastic moment of a steel tube section

$$N_k = \frac{\pi^2 (\frac{E'_c I_c}{5} + E_s I_s)}{l_k^2} \tag{37}$$

$$E'_c = (3.32\sqrt{F_c} + 6.90) \times 10^3 \tag{38}$$

$$C_M = 1 - 0.5(1 - \frac{M_1}{M_2})\sqrt{\frac{N}{N_k}} \geq 0.25 \quad \text{for sidesway prevented}$$
$$C_M = 1 \quad \text{for sidesway permitted} \tag{39}$$

M_1 , M_2: end moments, M_2 being numerically larger one. M_1 / M_2 is positive when the member is bent in single curvature, and negative when it is bent in reverse curvature.

$$C_b = 0.923 - 0.0045 F_c \tag{40}$$

In Eqs. (38) and (40), the value of F_c should be given in N/mm^2. Equations (32) and (33) are derived from the concept that the *M-N* interaction curve for a long composite column is given by superposing two *M-N* interaction curves separately computed for a long concrete portion and a long steel portion, which was proposed by Wakabayashi[45, 46]. *M-N* interaction formulas used here for the concrete portion and the steel potion are given by Eqs. (34) and (36), respectively, shown before. Equation (34) is newly proposed in Ref. [9], and Equation (36) is well-known and worldwide design formula for steel beam-columns. A simple superposition of these two interaction curves contains the conflict that the deformations of the concrete portion and the steel portion do not coincide. The term ($1 - N/N_k$) appearing in Eqs. (32) and (33) takes care of additional $P\delta$ effect generated by making two deformations coincide.

Equation (32) corresponds to the case that the axial load N is small enough to be carried by the concrete portion only, and the total bending strength of a CFT beam-column is given by the sum of the remaining bending strength of the concrete portion and the bending strength of the steel portion. On the other hand, Eq. (33) corresponds to the case that the concrete portion carries the axial load equal to its full strength, since the axial load N is too large, and the steel portion carries the remaining axial load and bending. Details of Eqs. (32) ~ (40) and their accuracy are discussed in Ref. [9].

iii) Ultimate Tensile Strength of a Diaphragm

Ultimate strength of outer diaphragms subjected to tension from the adjacent beam flange is given by the following formulas:

For an outer diaphragm of a rectangular CFT (Fig. 32(a)):

$$P_u = 1.42\{2(4t + t_s) t F_1 + \frac{4}{\sqrt{3}} h_s t_s F_2\} \tag{41}$$

For an outer diaphragm of a circular CFT (Fig. 32(b)):

$$P_u = 1.42[1.53\{(0.63 + 0.88\frac{B_f}{D})\sqrt{Dt} + t_s\} t F_1 + 1.77 h_s t_s F_2] \tag{42}$$

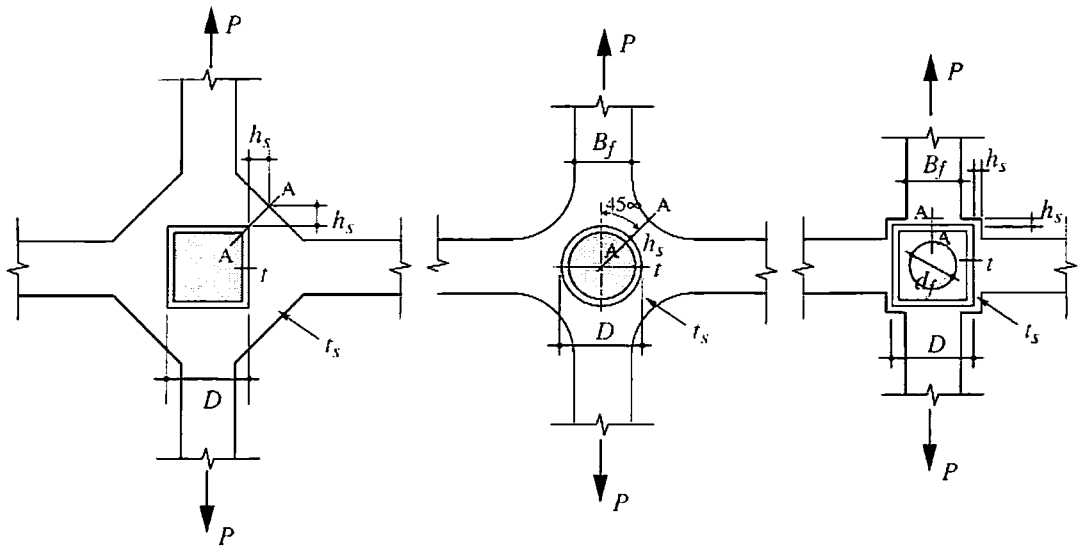

(a) Outer diaphragm (b) Outer diaphragm (c) Through diaphragm

Fig. 32 Design of Diaphragms

For a through diaphragm of a rectangular CFT (Fig. 32(c)):

$$P_u = 1.42\,(D + 2h_s - d_f)^2 \frac{B_f t_s}{d_f^2} F_2 \tag{43}$$

where

h_s : width of a diaphragm at A-A section

t_s : thickness of a diaphragm

B_f : width of a beam flange

d_f : diameter of an opening for concrete casting

F_1, F_2 : design standard strengths of steel tube and diaphragm, respectively

The ultimate strengths, Eqs. (41) ~ (43), were empirically obtained as 1.42 times the yield strength. The yield strengths in Eqs. (41) and (42) were derived based on the mechanism, in which the diaphragm plate at section A-A yields in tension and shear, and tube wall with an effective width yields in tension. The yield strength in Eq. (43) corresponds to the mechanism in which yielding occurs at section A-A of a fixed-end beam with width t_s, depth $(D + 2h_s - d_f)/2$ and length d_f under the load P/B_f distributed along the distance B_f at the center of the beam. Detailed derivation of Eqs. (41) and (43) is given in Ref. [47], and that of Eq. (42) in Ref. [48].

Formulas for a through diaphragm of a circular CFT and for an inner diaphragm have been derived by the yield line theory and experiments, although their expressions are very complicated[49, 50].

iv) Ultimate Shear Strength of a CFT Shear Panel

Figure 33(a) shows an internal beam-to-column connection with bending moments and shear forces acting at member ends, and shear forces Q_{pc} and Q_{pb} are acting on a CFT shear panel as resultant forces of member end forces. The ultimate strength of the shear panel Q^p_u to resist Q_{pc} is given by

$$Q^p_u = A_c \tau^c_u + \frac{A_s}{2} \tau^s_u \tag{44}$$

where

τ^c_u , τ^s_u : ultimate shear stresses of concrete and steel tube, respectively

Equation (44) gives the ultimate shear strength as a sum of the strengths of concrete and two webs of steel tube, and it is applicable to the circular CFT shear panel. The ultimate shear stresses are given as follows:

$$\tau^c_u = \beta \times min\,(0.12 F_c\,,\ 1.8 + 0.036 F_c) \tag{45}$$

$$\tau_u^s = \frac{1.2}{\sqrt{3}} F_s \qquad (46)$$

where

$$\beta = 2.5 \frac{D}{d_b} \text{ and } \leq 4 \text{ for a square CFT shear panel}$$

$$\beta = 2.0 \frac{D}{d_b} \text{ and } \leq 4 \text{ for a circular CFT shear panel} \qquad (47)$$

In Eq. (45), the value of F_c should be given in N/mm^2. The shear force acting on filled concrete may be actually resisted by the horizontal force carried by a diagonal strut forming in the shear panel, and it becomes larger as the inclination angle of the strut becomes smaller, in other words, the value of D/d_b becomes larger. The parameter β considers this effect.

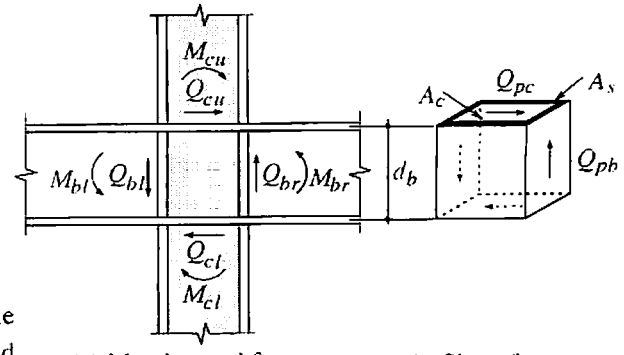

(a) Member end forces (b) Shear forces on the panel

Fig. 33 Shear Panel

The panel shear force Q_{pc} caused by the member end forces is approximately given by

$$Q_{pc} = \frac{M_{bl} + M_{br}}{d_b} \frac{h'}{h} \qquad (48)$$

where

M_{bl}, M_{br}: bending moments at beam ends adjacent to the shear panel

h, h': center-to-center story height and clear story height, respectively

6. COST MERIT INVESTIGATION BY TRIAL DESIGN OF CFT COLUMN SYSTEM

As mentioned in the Sect. 3.1.3, trial designs were performed for 10-, 24- and 40-story building frames using CFT column system, as a part of the work in the fifth phase of the U.S.-Japan Cooperative Earthquake Research Program, to investigate the merits of the CFT system, by comparing constructional costs and structural performance with those of the ordinary steel system. This work was done by the design team consisting of design practitioners who participated in the US-Japan Program, and is summarized as follows.

6.1 Theme Structures and Trial Design

6.1.1 Theme Structures

Theme structures treated here are 10-, 24- and 40-story unbraced building frames made of CFT or Steel(S) system, as shown in Fig. 34. A typical floor plan is shown in Fig. 35, which is common for all six theme structures designed. CFT or steel tube is used for columns, and H-shaped steel is used for beams. All beam-to-column connections are designed as moment connections, and thus moment resisting

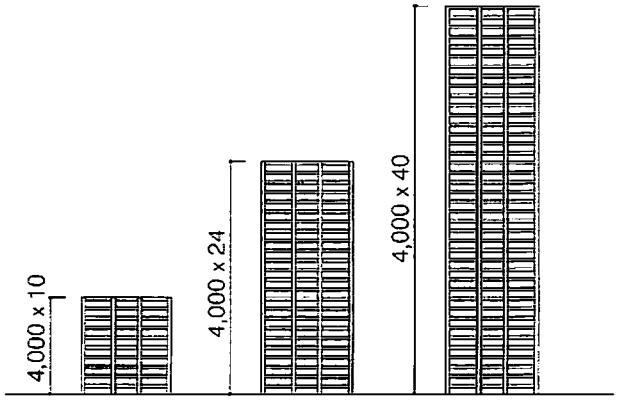

Fig. 34 Framing Elevations

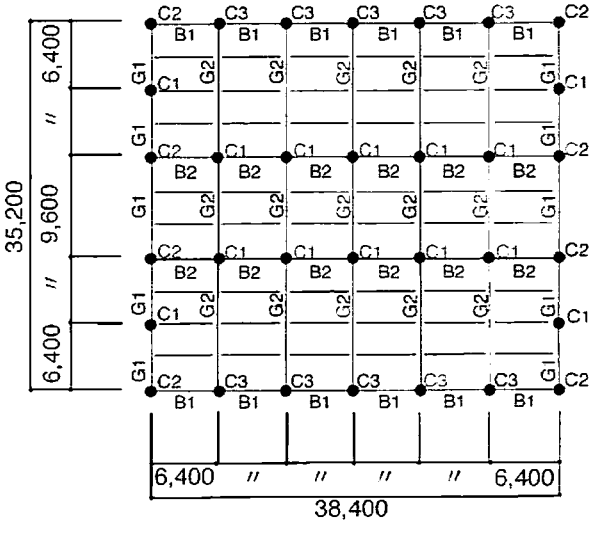

Fig. 35 Framing Floor Plan

frames are used for both interior and exterior frames. The structural design was mainly based on the design provisions in Structural Requirements of Building Center of Japan (BCJ)[5] and CFT Guidelines[6]. All frames were first designed by the allowable stress design against the seismic shear force under moderate earthquake, and the ultimate horizontal strength was calculated by the pushover analysis, and it was verified that the strength of each story exceeded the required value. In the course of design, each member was proportioned in such a way that the plastic hinges mainly formed in beams, and the columns remained elastic until the mechanism state was reached, except for a few cases such as the column bases in the 1st story.

In a conventional seismic design of a building structure, the concept of weak beam and strong column has been adopted to avoid damage concentration to a specific story. Thus, the following design conditions were adopted in this study: i) The ratio of the stress in the column caused by the design load to the allowable stress was kept as near to 0.8 as possible, and that of the beam as near to 1.0 as possible; ii) Story drift angles were kept within 1/200 under the design load in the allowable stress design; and iii) The collapse mechanism at the ultimate state was the overall frame mechanism in which the plastic hinges formed only in beams, and all columns remained elastic except for the specific part such as the bottom ends of columns in the 1st story. The material strength employed were as follows: yield strength of steel = 325 MPa; design standard strength of concrete = 36 MPa for 10-story building, and 72 MPa for 24- and 40-story buildings, respectively.

In order to check the structural characteristics of the designed frames, the elasto-plastic pushover analysis was performed for each frame with the following treatments and assumptions: i) Bending and shear deformations were considered for all members, and in addition, axial deformations for columns. ii) Floor of each story was assumed as a rigid horizontal diaphragm. iii) Stiffness of CFT columns was calculated as a simple sum of stiffness of steel and concrete. iv) Moment-rotation relation assumed for beam-ends was normal bi-linear, which changed the stiffness at the full plastic moment, having the second stiffness equal to 1/100 of the first. v) Moment-rotation relation assumed for column-ends was normal tri-linear[6], which changed the stiffness at yield moment and at the full plastic moment. 3-dimensional analysis by stiffness matrix method was used.

6.2 Characteristics of Designed CFT and Steel Frames

Weight and stiffness of 40-story frames revealed the following characteristics: i) weight of CFT columns: CFT/S = 2.1 ~ 3.3; ii) cross-sectional axial stiffness: CFT/S = 1.5 ~ 2.2; iii) cross-sectional bending stiffness: CFT/S = 1.1 ~ 1.5; iv) story weight: CFT/S = 1.1 ~ 1.16; and v) story shear stiffness: CFT/S = 1.1 ~ 1.3.

Figure 36 shows each story displacement of CFT frames and components caused by the bending and shear

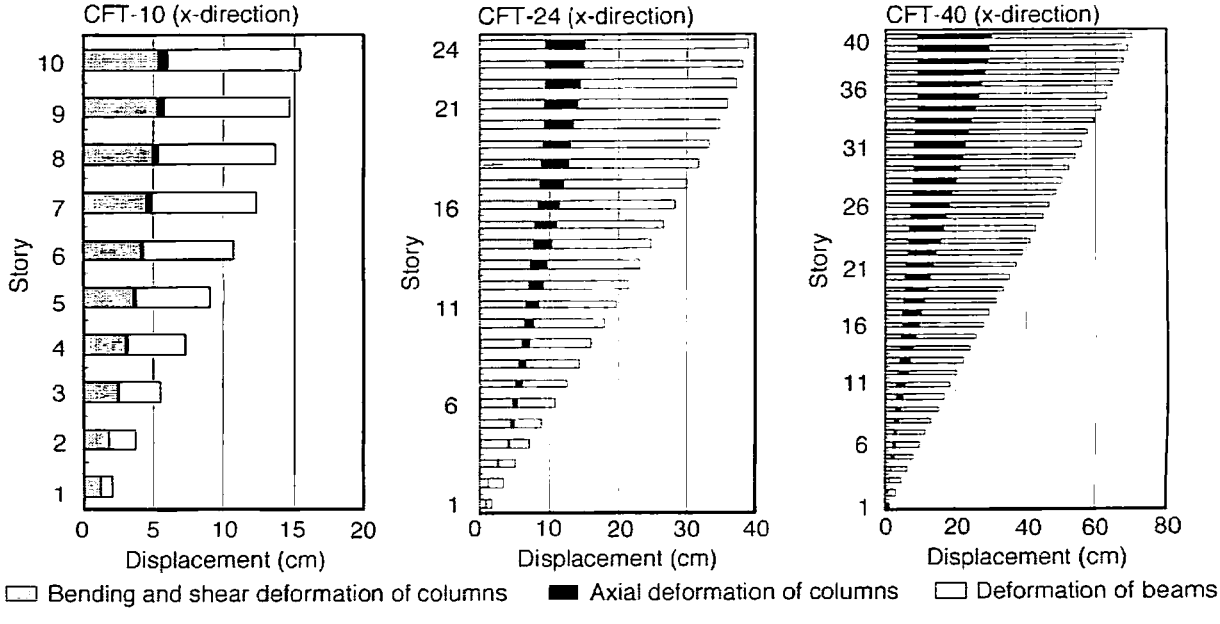

Fig. 36 Proportions of Each Story Displacement Caused by Beam and Column Deformations

deformations of beams and the bending, shear and axial deformations of columns. It is observed from Fig. 36 that 60 to 70 % of the total story displacement is caused by the beam deformation and the rest is caused by the column deformations in all cases of 3 frames analyzed. The proportion of axial deformation of the column to the total story displacement increases as the number of story increases, and it becomes as large as 30 % in the case of the 40-story frame.

Natural periods were calculated by the elastic eigenvalue analysis of the lumped mass model with 3 degrees of freedom which modeled the designed frame. The stiffness in each story was determined from the full stiffness matrix in the elastic range obtained in the pushover analysis. Table 3 shows the 1st natural period of vibration. There is only 2 % difference between CFT and S systems. This is because the weight ratio and the lateral stiffness ratio between CFT and S systems are almost the same.

Figure 37 shows the relations between the story shear Q and the story drift δ at 2nd and 9th stories of the 40-story frames. The following observations are made: i) Yielding story shear forces of CFT and S systems are almost the same, because the overall frame mechanism with beam hinges was adopted. ii) Energy absorbed in one story of the CFT system at drift angle 1/100 is larger by 4 to 8 % than that of the S system.

6.3 Amount of Steel and Cost Estimation

Figure 38 shows the comparison of steel amount per unit floor area used for the CFT and S systems, and its ratio. Total steel amount includes steel used for the columns, beams and sub-beams for entire building. Plates and bolts for connections and reinforcing bars for floor slabs, foundation beams and footings are not included, which may be almost the same in both the CFT and S systems. The following results were obtained: i) total steel amounts per unit floor area of the S frames were 105 kg/m^2 for the 10-story frame, 143 kg/m^2 for the 24-story frame and 189 kg/m^2 for the 40-story frame. These numbers are within a reasonable range compared with those in the existing buildings; ii) steel amount of CFT columns is about 25 % less than that of S columns, and the total steel amount of the CFT system is about 10 % less than that of the S system.

Table 3 1st Natural Period

Frame	System	Tx(sec)	Ty(sec)
10-story frame	CFT	1.37	1.42
	S	1.39	1.43
	CFT/S	0.99	0.99
24-story frame	CFT	2.64	2.71
	S	2.70	2.75
	CFT/S	0.98	0.98
40-story frame	CFT	3.73	3.80
	S	3.72	3.80
	CFT/S	1.00	1.00

Table 4 shows a cost estimation of main frames including columns, beams and sub-beams. The unit cost was assumed to be 250,000 Japanese yens per ton for steel,

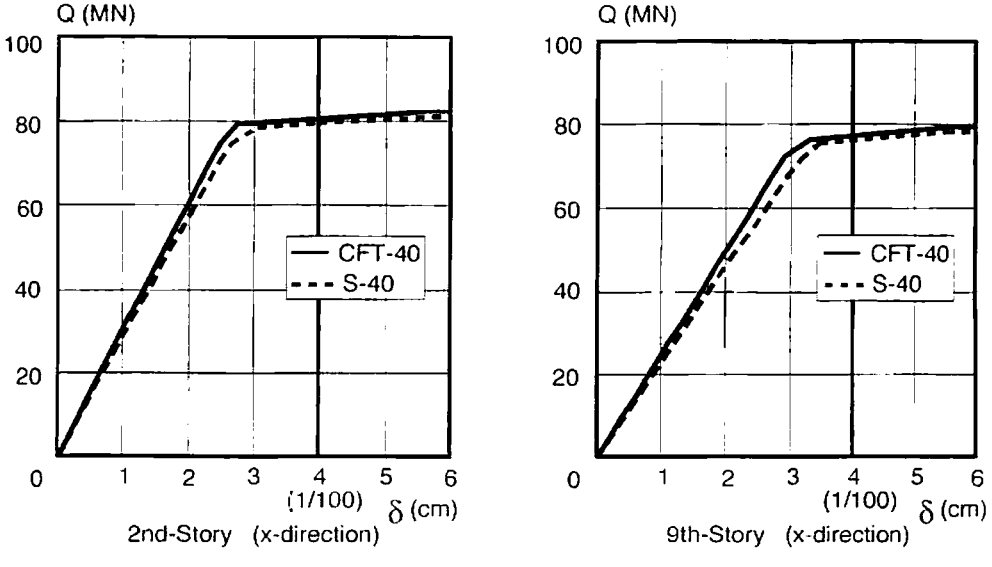

Fig. 37 Load-Deflection Relations of 40-Story Frames

and 35,000 yens per cubic meters for concrete. These unit costs include materials, fabrications, transportation, and constructions. The cost merits provided from the savings in the construction time and manpower were not precisely considered, but it is observed that: i) cost of the CFT main frames is 5 to 7 % lower than that of the S frames.; ii) total building cost for the CFT system would be 1 % lower than that of the S system, if the cost of main frame structure is assumed to occupy 15 % of the total building cost; and iii) as the number of stories increases, the cost merit of the CFT system becomes larger.

7. CONSTRUCTION OF CFT COLUMN SYSTEM IN JAPAN

The Association of New Urban Housing Technology (ANUHT) established in 1996 in relation to NUHP has been inspecting the structural and fire resistance designs of newly planned CFT buildings shorter than 60m and authorizing the construction of those structures. In addition to these inspection works, the ANUHT provides CFT system design and construction technology, educates the member companies, and promotes the research on the CFT system. The construction data shown below are provided by the ANUHT.

Structural designs of 175 CFT buildings were inspected by the ANUHT from April, 1998 to March 2002, and their statistical details are shown in Figs. 39 and 40. Some of the data are missing for the buildings inspected before this period, and little data exists after this period, because the inspection work has been done outside the ANUHT since the publication of Notification No. 464. The Ministry of Land, Infrastructure and Transport, Japan initiated CFT construction technology by creating this notification on the structural safety of the CFT column system in 2002. For buildings taller than 60m, inspection has been done by the Building Center of Japan. More than 100 CFT buildings taller than 60m may have been constructed, but the construction database is not available.

Observations made from the data for the CFT buildings shorter than 60m are as follows:

Table 4 Cost Estimation of Main Frames

Frame	System	Amount of steel (t)	Amount of concrete (m^3)	cost (Japanese yen)
10-Story frame	CFT	1283	454	336,640,000
	S	1414	0	353,500,000
	CFT/S	0.91	-	0.95
24-Story frame	CFT	4186	1379	1,094,765,000
	S	4653	0	1,163,250,000
	CFT/S	0.90	-	0.94
40-Story frame	CFT	9148	2905	2,388,675,000
	S	10221	0	2,555,250,000
	CFT/S	0.90	-	0.93

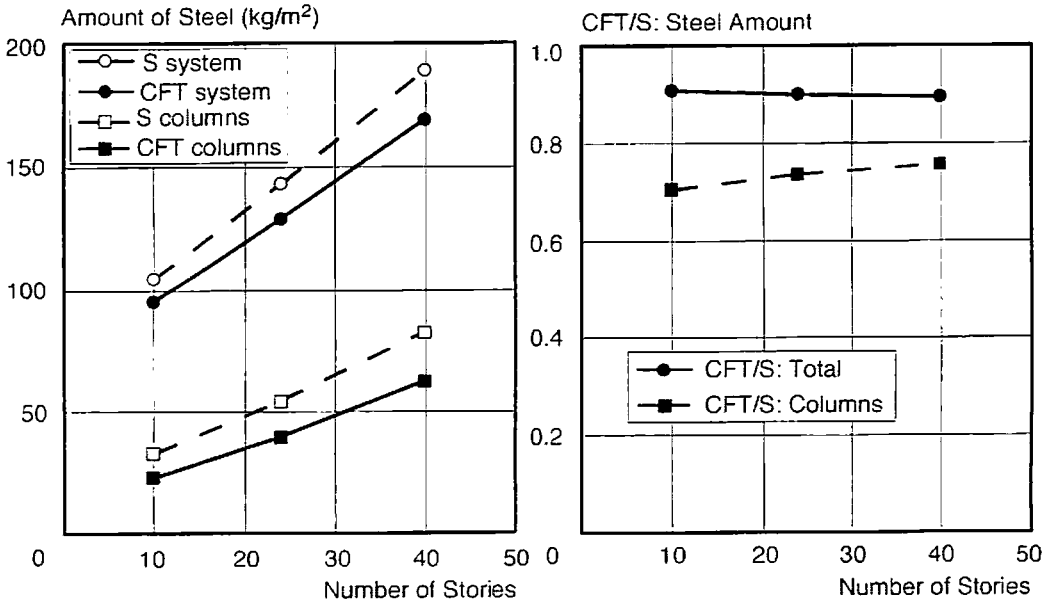

Fig. 38 Comparison of Steel Amount between CFT and Steel Frames

1) Among 175 buildings, 65% are shops and offices, and their total floor area constitutes about 60% of the total floor space (Figs. 39(a), (b)). Application of CFT to those buildings indicates the building designer's recognition of the effectiveness of the CFT system for long spans in buildings with large open spaces. The CFT system is quite often applied to buildings of large scale (Figs. 40(a)~(c)).

2) The CFT system is not very often applied to braced frame buildings (Fig. 39(c)). It may not be necessary to use the braces, since the tube section has identical strength and stiffness in both x- and y-directions. It is also not very common to use structural walls with the CFT system.

3) The floor area supported by one column is much larger than in ordinary reinforced concrete or pure steel buildings. The floor area per column exceeds 90 m^2 in about 40% of all buildings, and in about 40% of office buildings (Figs. 39(d), (e)). This emphasizes again application of the CFT system to buildings with large open spaces.

4) A wide variety of aspect ratio (ratio of the longer distance between two columns to the shorter one in x- and y-directions of a floor plan) of span grids in Figs. 39(f) and (h) indicates the CFT system's potential for free planning about the span grid. In the case of office buildings, a rectangular span grid of 8m x 18m is fairly often used, and the aspect ratio exceeds 2.2 (about 40% of cases), while the span grid of shop buildings is fairly close to square (about 50% of cases).

5) Both square and circular sections are used together in a number of buildings (Fig. 39(g)). The size of the tube section often used is between 500 and 700 mm in the case of square CFT columns (about 80% of cases), and 500 and 711 mm

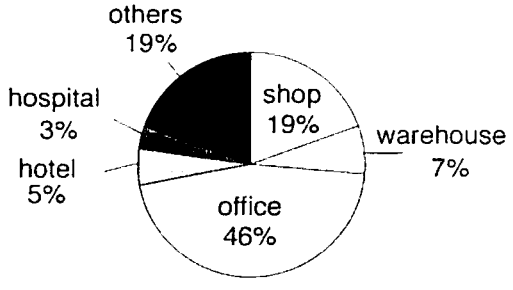

(a) Number of constructions and use

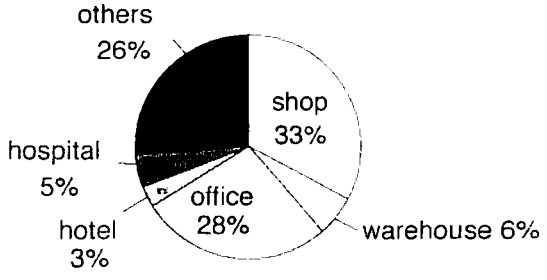

(b) Total floor area and use

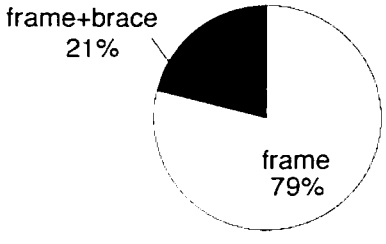

(c) Type of structural frames

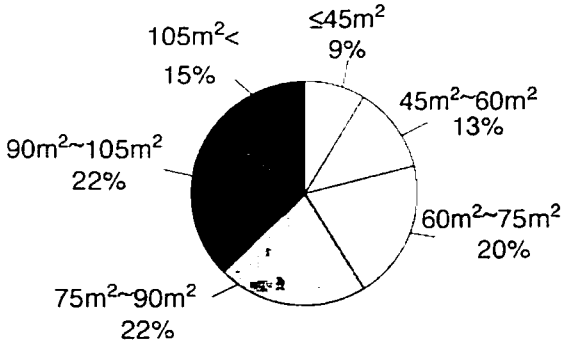

(d) Floor area carried by one column

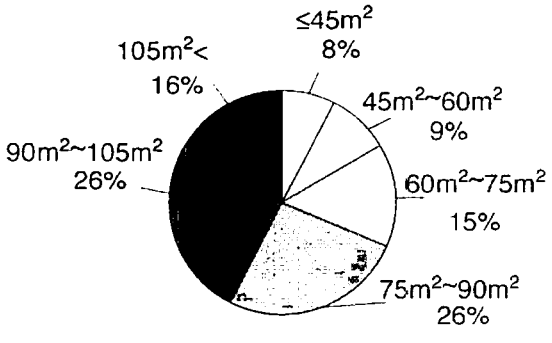

(i) Offices

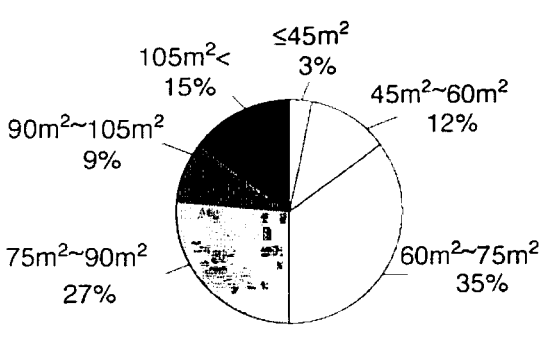

(ii) Shops

(e) Floor area carried by one column of offices and shops

Fig. 39 Costruction Data in 1998-2002: Structural Planning

in the case of circular CFT columns (about 65% of cases) (Figs. 40(e), (f)). Circular tubes (diameter: 400 to 1117 mm, diameter-thickness ratio: 16 to 90) are mainly used for buildings with irregular plan grids, and square and rectangular tubes (width: 300 to 950 mm, width-thickness ratio: 10 to 54) are used for the case of regular plans. Most tubes are cold-formed, since they are inexpensive and widely available. Box sections built-up by welding are used when the plate becomes thick and/or large ductility is required. Cast-steel tubes are used to simplify the beam-to-column connection. Annealing to remove residual stresses is scarcely done in Japan.

6) Inner or through diaphragms are used in most beam-to-column connections (about 80% of cases) (Fig. 39(i)). The type of diaphragm used seems to be determined by the plate thicknesses of the column and the beam: the through diaphragm is often employed when the beam flange is thicker than the column skin plate; otherwise the inner diaphragm is employed. The through diaphragm is usually used for cold-formed tubes and the inner diaphragm for built-up tubes. Inner and through diaphragms have openings with diameter of 200 to 300 mm for concrete casting, and several small holes for air passage. The outer diaphragm is used as an easy solution, which ensures compaction of the concrete.

7) Embedded column bases are the most widely used (about 60% of cases), as they are the most structurally reliable (Fig. 39(j)). This trend also indicates that the CFT system is often applied to large-scale buildings. If the building has basement stories, encased column bases are often employed, in which column tube sections are changed to cross-H sections, and CFT columns become concrete encased steel columns in the basement.

8) The ratio of the column effective length to the column depth is much larger than that in ordinary reinforced concrete

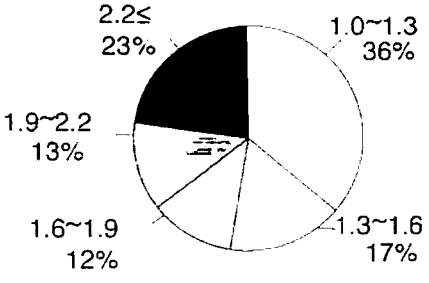

(f) Aspect ratio of span grid

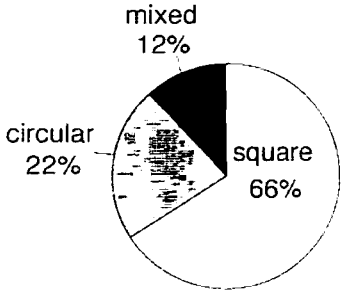

(g) Shape of steel tubes

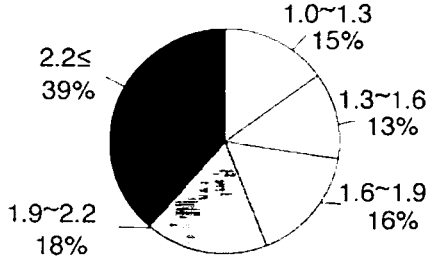

(i) Offices

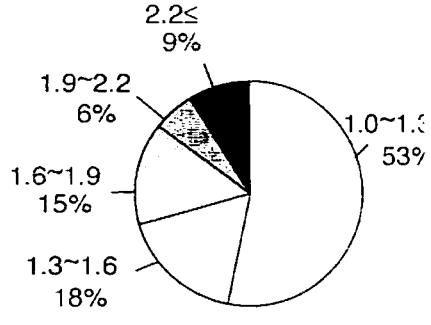

(ii) Shops

(h) Aspect ratio of span grid of offices and shops

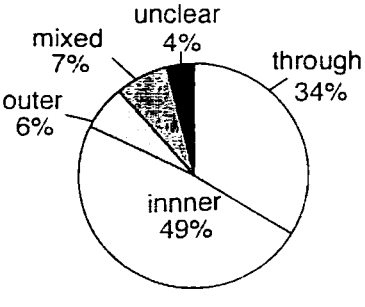

(i) Type of beam-to-column connections

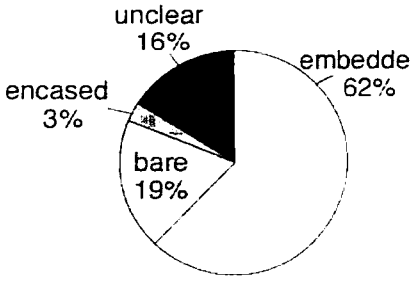

(j) Type of column bases

Fig. 39 Costruction Data in 1998-2002: Structural Planning (continued)

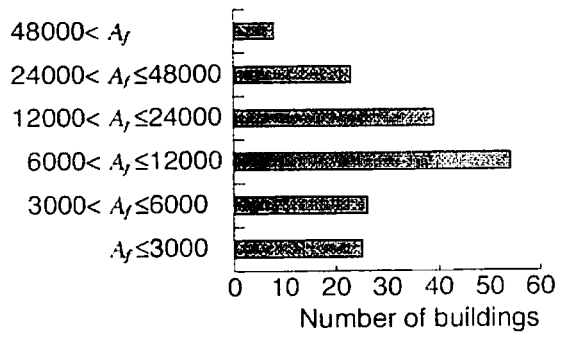

(a) Total floor area(A_f : m²)

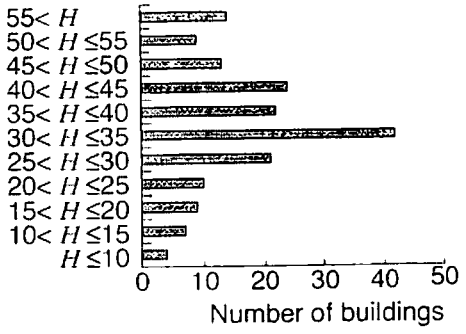

(b) Height of buildings(H : m)

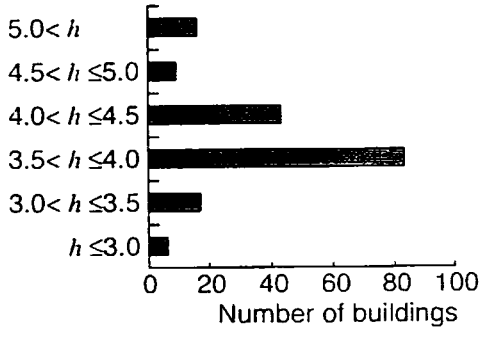

(c) Height of typical story (h : m)

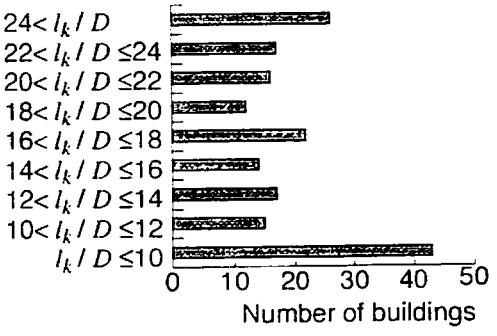

(d) Ratio of buckling length(l_k) to tube size(D)

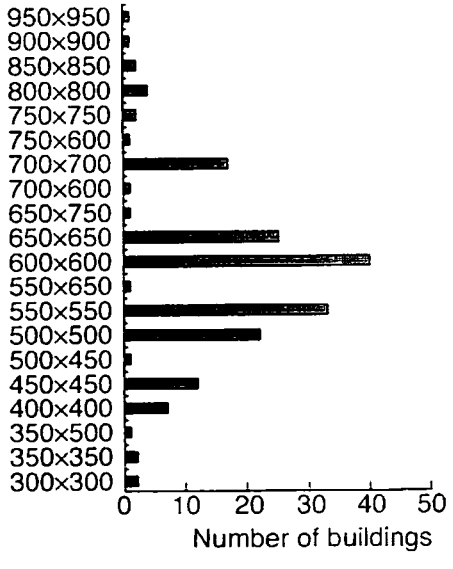

(e) Size of square tubes (mm)

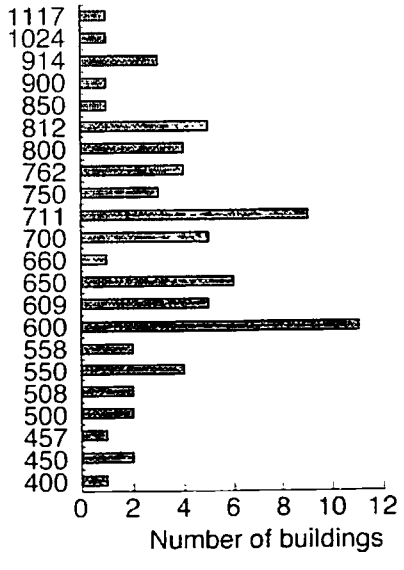

(f) Size of circular tubes (mm)

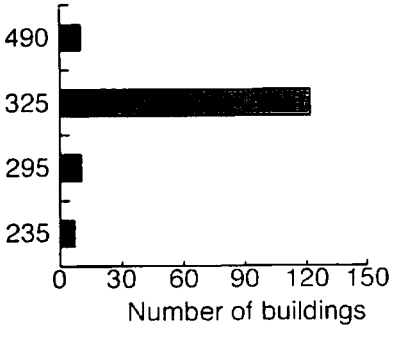

(g) Design standard strength of steel (MPa)

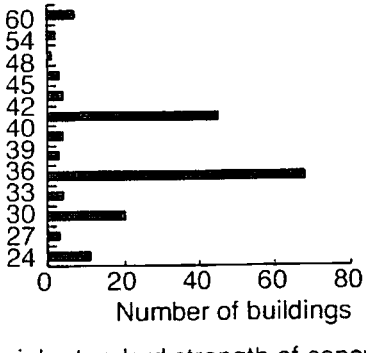

(h) Desigh standard strength of concrete (MPa)

Fig. 40 Costruction Data in 1998-2002: Properties of CFT Systems and Columns

or pure steel buildings (Fig. 40(d)). This difference indicates the relatively large axial load-carrying capacity of the CFT column.

9) The design standard strength of steel most often used is 325 MPa (about 85% of cases), and that of concrete is 36 and 42 MPa (about 65% of cases) (Figs. 40(g), (h)).

8. CONCLUDING REMARKS

A rational design method for the CFT column system has been established through extensive research by the Architectural Institute of Japan, the New Urban Housing Project and the U.S.-Japan Cooperative Earthquake Research Program, and several design standards, recommendations and guidelines are available[2, 3, 5, 6]. Enabling an engineer to design a CFT column system freely requires, i) a design method for a CFT beam-column using higher strength material, ii) formulas to evaluate deformation capacity of both short and long beam-columns, iii) the restoring force characteristics of a CFT beam-column and connection, and iv) the limiting value of design compressive force taking structural properties of a CFT column into consideration.

More than 40 buildings have been constructed each of the last five years in Japan. CFT structures are mainly used in shop, office and hotel construction. The characteristics of CFT make the system especially applicable to high-rise and long-span structures, because the system's construction efficiency saves construction cost, time and manpower. Trial designs of unbraced frames have shown that the structural characteristics of the CFT and steel systems are almost the same, but the total steel consumption of the CFT system for entire building is about 10 % less than that of the steel system.

The deformation at which a CFT beam-column reaches the maximum strength is fairly large: some of the specimens attained the maximum strength after the chord rotation angle became larger than 1/100. In addition, it becomes known that the dynamic characteristics of the CFT system are almost the same as those of the steel system. These facts indicate that the CFT system is not very stiff against lateral loads, and thus, further investigation of structural systems other than moment frames is now needed in order to utilize the large axial load-carrying capacity of the CFT column more effectively. Other lateral resisting systems may include braced frames or a combination of reinforced concrete shear walls and CFT columns in which CFT columns carry most of the vertical load.

The weak point of the CFT system is the connections: beam-to-column connections, brace-to-frame connections and column bases. The outer diaphragm type of beam-to-column connection is sometimes avoided because the diaphragm sticking outward disturbs the arrangement of curtain walls, so the through type of connection is most popular. The through diaphragm type of connection is fabricated by first cutting the steel tube into three pieces and then welding them together with two diaphragms, as shown in Fig. 41(a). Therefore, the type requires a large amount of welding. Moreover, if the heights of beams coming into a connection are different, or a brace is attached to a CFT column with a gusset plate and diaphragms, filled concrete in the tube is separated into more layers than in an ordinary beam-to-column connection, as shown in Figs. 41(b) and (c). These cases require a greater amount of welding and

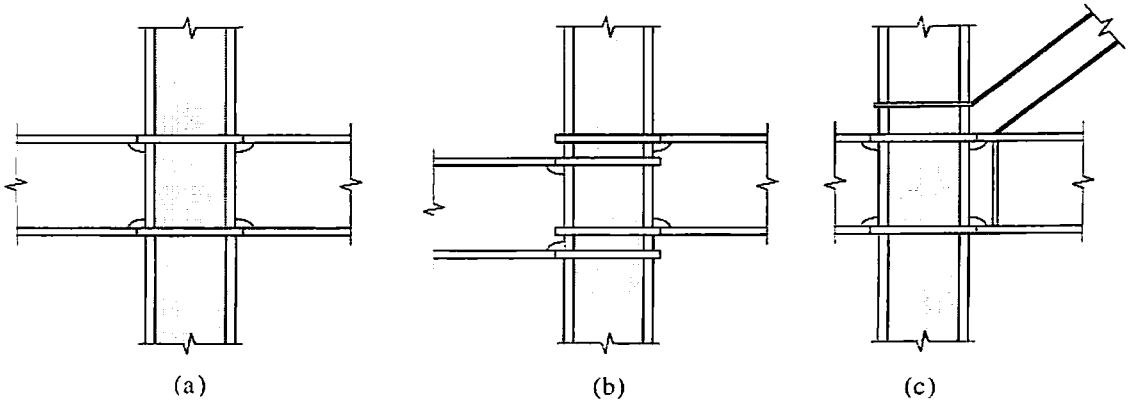

Fig. 41 Arrangement of Diaphragms

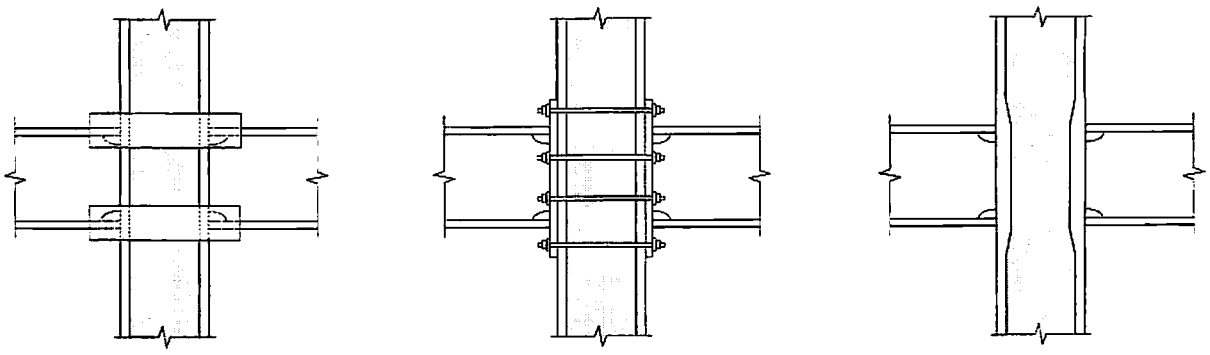

(a) Vertical stiffener (b) Long bolts (c) Increased thickness

Fig. 42 Connections without Diaphragms

increase the possibility of defects in cast concrete. Therefore, development of a new type of connection without cutting the column body and without using welding is needed. A possible alternative is a connection that uses vertical stiffeners[14], long bolts[15, 16] or a steel tube whose wall thickness is partly increased at the connection[17], as shown in Fig. 42. Some research work has been done on these new types, but design formulas are not yet well prepared.

The CFT column base is usually designed by the same way as an ordinary steel column base, without any special consideration. For example, in the design of a bare type CFT column base, it is assumed that total axial load and bending moment are resisted by the tensile strength of the anchor bolts, bending strength of the base plate, and the bearing strength of the concrete foundation. The shear force is resisted by the friction between the base plate and the concrete, and the shear strength of the anchor bolts. However, some part of the compressive axial load may be directly transferred to the foundation concrete, and the concrete portion in the CFT column may be effective in resisting shear if it is continuous to the foundation concrete through an opening in the base plate. Therefore, a more suitable design method to utilize the CFT characteristics may be possible. Investigation on this subject has just started.

Most design engineers have treated the CFT system as an alternative to the steel system, trying to cut the cost by reducing the steel consumption. However, it is also possible to look at the CFT system as an alternative to the reinforced concrete system. In addition to structural advantages such as high strength and high ductility, the CFT system has the following ecological advantages over the RC system: neither formwork nor reinforcing bars are needed, which leads to very clean construction site; steel tube peels from the filled concrete and is reused when the building is pulled down; filled concrete is of high quality and is easily crashed because it does not contain reinforcing bars, and therefore is also reusable as aggregates. An unanswered question regarding the effectiveness of the CFT column system is its overall cost performance, and thus, investigation by trial design is needed to compare the advantages and disadvantages of the CFT system with the RC system, including life cycle assessment.

ACKNOWLEDGMENTS

The work introduced in Chapter 6 has been done by the members of the CFT Subcommittee under the supervision of Japan Technical Coordinating Committee (Chairman: Prof. Hiroyuki Aoyama, Nihon University, Prof. Emeritus of the University of Tokyo) for U.S.-Japan Cooperative Earthquake Research Program, in close cooperation with Building Research Institute, Building Center of Japan, Building Contractor's Society, Japan Structural Consultants Association, Kozai Club (Japan Iron & Steel Exporters' Association), Kyushu University and Mie University. Construction data presented in Chapter 7 were generously provided by the Association of New Urban Housing Technology. The authors wish to express sincere gratitude to the members of these committees, cooperative organizations and the Association.

REFERENCES

[1] Standards for Structural Calculation of Steel Reinforced Concrete Structures, English Ed., Architectural Institute of Japan(AIJ), 1991.9.

[2] Standard for Structural Calculation of Steel Reinforced Concrete Structures, 5th Ed., AIJ, 2001.1. (in Japanese)
[3] Recommendations for Design and Construction of Concrete Filled Steel Tubular Structures, AIJ, 1997.10. (in Japanese)
[4] Reports of Committee for Evaluation of Structural Performance of Concrete-Filled Steel Tubular Columns, Building Center of Japan(BCJ), 1989.3. (in Japanese)
[5] Design Recommendations for Concrete-Filled Steel Tube Structures, Association of New Urban Housing Technology, 2000.8. (in Japanese)
[6] Guidelines for the Structural Design of CFT Column System (draft), BCJ, 1998.10. (in Japanese)
[7] Nishiyama, I. Morino, S., Sakino, K., et al.: Summary of Research on Concrete-Filled Structural Steel Tube Column System Carried out under the US-Japan Cooperative Research Program on Composite and Hybrid Structures, BRI Research Paper No. 147, 2002.1
[8] Sakino, K. Ninakawa, T. Nakahara, H. and Morino, S.: Experimental Studies and Design Recommendations on CFT Columns - U.S.-Japan Cooperative Earthquake Research Program -, Proc. Structural Engineers World Congress, San Francisco, CD Rom, Paper No. T169-3, 1998.7.
[9] Tsuda, K., Matsui, C. and Fujinaga, T.: Simplified Design Formula of Slender Concrete-Filled Steel Tubular Beam-Columns, Proc. 6th ASCCS Conference on Composite and Hybrid Structures, Los Angeles, Vol. 1, pp. 457-464, 2000.3.
[10] Nakahara, H., Sakino, K. and Inai, E.: Analytical Model for Compressive Behavior of Concrete Filled Square Steel Tubular Columns, Transactions of Japan Concrete Institute, Vol. 20, pp. 171-178, 1998.6.
[11] Nakahara, H. and Sakino, K.: Flexural Behavior of Concrete Filled Square Steel Tubular Beam-Columns, Proc. 12th WCEE, Auckland, CD-Rom, No. 1923, 2000.1.
[12] Sakino, K., Inai, E. and Nakahara, H.: Tests and Analysis on Elasto-Plastic Behavior of CFT Beam-Columns -U.S.-Japan Cooperative Earthquake Research Program-, Proc. 5th Pacific Structural Steel Conference, Seoul, Vol. 2, pp. 901-906, 1998.10.
[13] Inai, E., Noguchi, T. Mori, O. and Fujimoto, T.: Deformation Capacity and Hysteretic Model of Concrete-Filled Steel Tubular Beam-Columns, Proc. 6th ASCCS Conference on Composite and Hybrid Structures, Los Angeles, Vol. 1, pp. 605-612, 2000.3.
[14] Kawano, A. and Matsui, C.: New Connections Using Vertical Stiffeners and Hollow or Concrete-Filled Square Tubular Columns, Proc. Engineering Foundation Conference on Composite Construction in Steel and Concrete III, Irsee, pp. 172-185, 1996.6.
[15] Kanatani, H., Tabuchi, M., Kamba, T., Ji, H. and Ishikawa, M.: A Study on Concrete Filled RHS Column to H-Beam Connections Fabricated with HT Bolts in Rigid Frames, Proc. Engineering Foundation Conference on Composite Construction in Steel and Concrete, Henniker, pp. 614-635, 1987.7
[16] Ji, H., Kanatani, H., Tabuchi, M., Kamba, T. and Ishikawa, M.: Behavior of Concrete Filled RHS Column to H-beam Connections Fabricated with HT Bolts, Tubular Structures III, Proc. 3rd International Symposium on Tubular Structures, Lappeenranta, pp. 196-203, 1989.9.
[17] Morita, K., Ebato, K., Furuhara, K., Fujita, K. and Hamano, K.: Experimental Study of Structural Behavior of Beam-to Column Connections Reinforced by Increasing Plate Thickness of Column without Diaphragms, Tubular Structures VIII, Proc. 8th International Symposium on Tubular Structures, Singapore, pp. 585-594, 1998.8.
[18] Fukumoto, T. and Morita, K.: Elasto Plastic Behavior of Steel Beam to Square Concrete Filled Steel Tube (CFT) Column Connections, Proc. 6th ASCCS Conference on Composite and Hybrid Structures, Los Angeles, Vol. 1, pp. 565-572, 2000.3.
[19] Fujimoto, T., Inai, E., Kai, M., Mori, K., Mori, O. and Nishiyama, I.: Behavior of Beam-to Column Connection of CFT Column System, Proc. 12th WCEE, Auckland, CD-Rom, No. 2197, 2000.1.
[20] Kawaguchi, J. Morino, S. and Sugimoto, T.: Elasto-Plastic Behavior of Concrete-Filled Steel Tubular Frames, Proc. Engineering Foundation Conference on Composite Construction in Steel and Concrete III, Irsee, pp. 272-281, 1996.6.
[21] Uchikoshi, M. Hayashi, Y. and Morino, S.: Merits of CFT Column System -Results of Trial Design of Theme Structures-, Composite and Hybrid Structures, Proc. of 6th ASCCS Conference, Los Angeles, pp.135-142, 2000.3.
[22] Kimura, M., Ohta, H., Kaneko, H. and Kodaira, A.: Fire Resistance of Concrete-Filled Square Steel Tubular Columns Subjected to Combined Load, Journal of Structural and Construction Engineering, Transaction of AIJ, No. 417, pp. 63-70, 1994.4. (in Japanese)
[23] Saito, H. and Saito, H.: Fire Resistance of Concrete-Filled Square Steel Tubular Columns under Deformation to

Simulate the Elongation of Steel Beams, Journal of Structural and Construction Engineering, Transaction of AIJ, No. 458, pp. 163-169, 1990.11. (in Japanese)
[24] J. Kawaguchi, S. Morino, T. Machida: Energy Dissipation Capacity of CFT Beam Columns Failing in Local Buckling, Proc. International Conference on Behavior of Steel Structures in Seismic Areas, Kyoto, pp.311-318, 1997.8.
[25] J. Kawaguchi, S. Morino: Experimental Study on Post-Local Buckling Behavior of CFT Beam-Columns under Cyclic Loading -Elasto-Plastic Behavior of Square CFT Beam-Columns Part 1-, Journal of Structural and Construction Engineering, Transactions of AIJ, No. 540, pp.141-148, 2001.2.
[26] J. Kawaguchi, S. Morino, T. Sugimoto and J. Shirai: Study on Elasto-Plastic Behavior of Portal Frames Consisting of Square CFT Columns, Journal of Constructional Steel, Vol. 5, pp.101-108, 1997.11.
[27] J. Kawaguchi, S. Morino, T. Sugimoto, J. Shirai: Experimental Study on Structural Characteristics of Portal Frames Consisting of Square CFT Columns, Proc. United Engineering Foundation Conference on Composite Construction in Steel and Concrete IV, Bannf, pp.725-733, 2000.5.
[28] S. Morino, J. Kawaguchi, C. Yasuzaki, S. Kanazawa: Behavior of Concrete-Filled Steel Tubular Three-Dimensional Subassemblage, Proc. Enginnering Foundation Conference on Composite Construction in Steel and Concrete II, Potosi, Missouri, pp.726-741, 1992.6
[29] J. Kawaguchi, S. Morino: Experimental study on Elasto-Plastic Behavior of Three-Dimensional Frames Consisting of CFT Columns -Elasto-Plastic Characteristics of CFT Three-Dimensional Frames Part 1-, Journal of Structural and Construction Engineering, Transactions of AIJ, No. 541, pp.187-195, 2001.3.
[30] J. Kawaguchi, S. Morino, and A. Tsuji: Fundamental Behavior of CFT Semi-Embedded Type Column Base, Proc. of US-Japan Seminar on Advanced Stability and Seismicity Concept for Performance-based Design of Steel and Composite Structures, Kyoto, pp. 129-135, 2001.7
[31] S. Morino, J. Kawaguchi, A. Tsuji, H. Kadoya: Strength and Stiffness of CFT Semi-Embedded Type Column Base, Proc. International Conference on Advances in Structures, ASSCCA'03, Sydney, Vol. 1, pp. 3-14, 2003.6.
[32] S. Morino, J. Kawaguchi, Z.S. Cao: Creep Behavior of Concrete-Filled Steel Tubular Members, Proc. Engineering Foundation Conference on Composite Construction in Steel and Concrete III, Irsee, pp.514-525, 1996.6.
[33] S. Morino, J. Kawaguchi, C. Yamada: Buckling Strength of Concrete-Filled Steel Tubular Compression Members Affected by Creep of Concrete, Proc. 2nd International Symposium on Civil Infrastructure Systems, Hong Kong, pp.61-66, 1996.12.
[34] T. Yamamoto, J. Kawaguchi, S. Morino: Experimental Study on the Scale Effect on Compressive Behavior of Concrete-Filled Steel Tube Short Columns, Proc. United Engineering Foundation Conference on Composite Construction in Steel and Concrete IV, Bannf, pp.879-890, 2000.5.
[35] T. Yamamoto, J. Kawaguchi, S. Morino: Size Effect on Ultimate Compressive Strength of Concrete-Filled Steel Tube Short Columns, Proceedings of Structural Engineers World Congress 2002, Yokohama, CD-ROM, T1-2-f-1, pp. 1-8, 2002.10.
[36] T, Yamamoto, J. Kawaguchi, S. Morino: Experimental Study of the Size Effect on the Behavior of Concrete-Filled Circular Steel Tube Columns under Axial Compression, Journal of Structural and Construction Engineering, Transactions of AIJ, No. 561, pp.237-244, 2002.11. (in Japanese)
[37] J. Kawaguchi, S. Morino, J. Shirai, E. Tatsuta: Database and Structural Characteristics of CFT Beam-Columns, Proc. of 5th Pacific Structural Steel Conference, Vol. 2, Seoul, pp. 955-960, 1998.10
[38](56) J. Kawaguchi, M. Ueda, S. Morino: Elasto-Plastic Behavior of Concrete-Filled Steel Tubular Frames, Journal of Constructional Steel, Vol. 2, pp.25-32, 1994.11.
[39] J. Kawaguchi, S. Morino, M. Ueda: Analysis of Elasto-Plastic Behavior of Concrete-Filled Steel Tubular Three-Dimensional Subassemblages, International Conference on Structural Stability and Design, Sydney, pp.295-300, 1995.10.
[40] J. Kawaguchi, S. Morino, M. Ueda: Analytical Study on Ultimate Strength of Steel-Concrete Composite Sections under Biaxial Bending, Research Reports of the Faculty of Engineering, Mie University, Vol.21, pp.27-35, 1996.12.
[41] J. Kawaguchi, S. Morino, M. Ueda: Ultimate Strength of Steel-Concrete Composite Sections under Biaxial Bending, Proc. IABSE International Conference on Composite Construction - Conventional and Innovative, Innsbruck, pp.936-937, 1997.9.
[42] A. Tsuiki, J. Kawaguchi, H. Fukao, S. Morino: Analysis of Cyclic Behavior of CFT Beam-Columns Failing in Local Buckling, Proc. of 5th Pacific Structural Steel Conference, Vol. 2, Seoul, pp. 907-912, 1998.10.
[43] S. Morino, A. Tsuiki, J. Kawaguchi: Load-Deflection Analysis of Concrete-Filled Steel Tube Bean-Columns

Failing in Local Buckling, Proc. of the Seng-Lip Lee Symposium on Innovative Solutions in Structural and Geotechnical Engineering, Bangkok, pp.135-144, 1999.5.
[44] Recommendations for the Design of Plastic Design of Steel Structures, AIJ, 1975.9. (in Japanese)
[45] Wakabayashi, M.: A Proposal For Design Formulas of Composite Columns and Beam-Column, Preliminary Report, 2nd International Colloquium on Stability, Tokyo, pp. 65-87, 1976.9.
[46] Wakabayashi, M.: A New Design Method of Long Composite Beam-Columns, 2nd International Colloquium on Stability, Washington, pp. 65-87, 1977.3.
[47] Matsui, C.: Strength and Behaviour of Frames with Concrete Filled Square Steel Tubular Columns under Earthquake Loading, Proc. International Specialty Conference on Concrete Filled Steel Tubular Structures, Harbin, pp. 104-111, 1985.8.
[48] Kurobane, Y., Togawa, T. and Matsuo, O.: Beam-to-Concrete Filled Tubular Column Connection with Stiffener Rings, Part 1 ~ 3, Abstracts, Structure II, Annual Meeting of Architectural Institute of Japan, pp. 1275-1280, 1987.10.
[49] Ito, H., Fu, G., Nagata, M., Nakamura, H. and Morita, K.: Structural Behaviours of Connections between Concrete Filled Steel Tubular Column and Steel Beam, Part 1 and 2, Abstracts, Structure III, Annual Meeting of Architectural Institute of Japan, pp. 831-834, 1995.8. (in Japanese)
[50] Morita, K., Yokoyama, Y., Kawamata, Y. and Matsumura, H.: Effect of Inner Ring Stiffener on the Strength of Connection between Steel Beam and Concrete-Filled Square Tube Column, Journal of Structural and Construction Engineering, Transactions of AIJ, No. 422, pp. 85-96, 1991.4. (in Japanese)
[51] Structural Requirements for Buildings, Building Center of Japan, BCJ, 1997.12.